Synergistic cytotoxicity of dual PI3K/mTOR and FLT3 inhibition in FLT3-ITD AML cells.

Salihanur Darici[1,2*], Manuela Zavatti[1*], Luca Braglia[1,3], Benedetta Accordi[4], Valentina Serafin[4], Gillian A Horne[2], Lucia Manzoli[3], Carla Palumbo[1], Xu Huang[2]#, Heather G Jørgensen[2], Sandra Marmiroli[1]#.

1Cellular Signaling Unit, Section of Human Morphology, Department of Biomedical, Metabolic and Neural Sciences, University of Modena and Reggio Emilia, Modena 41125, Italy. 2Haemato-Oncology/Systems Medicine Group, Paul O'Gorman Leukaemia Research Centre, Institute of Cancer Sciences, University of Glasgow, Glasgow G12 0ZD, UK. 3Department of Biomedical and Neuromotor Sciences, University of Bologna, Bologna, Italy. 4Department of Woman and Child Health, Haemato-Oncology Laboratory, University of Padua, via Giustiniani 3 and IRP Città della Speranza, Corso Stati Uniti 4, 35128 Padua, Italy.

*These authors contributed equally to the work

#Author for correspondence: sandra.marmiroli@unimore.it, xu.huang@glasgow.ac.uk

Abstract

Acute myeloid leukemia (AML) is an aggressive hematopoietic malignancy, characterized by a heterogeneous genetic landscape and complex clonal evolution, with poor outcomes. Mutation at the internal tandem duplication of FLT3 (FLT3-ITD) is one of the most common somatic alterations in AML, associated with high relapse rates and poor survival due to the constitutive activation of the FLT3 receptor tyrosine kinase and its downstream effectors, such as PI3K signaling. Thus, aberrantly activated FLT3-kinase is regarded as an attractive target for therapy for this AML subtype, and a number of small molecule inhibitors of this kinase have been identified, some of which are approved for clinical practice. Nevertheless, acquired resistance to these molecules is often observed, leading to severe clinical outcomes. Therapeutic strategies to tackle resistance include combining FLT3 inhibitors with other antileukemic agents. Here, we report on the preclinical activity of the combination of the FLT3 inhibitor quizartinib with the dual PI3K/mTOR inhibitor PF-04691502 in FLT3-ITD cells. Briefly, we show that the association of these two molecules displays synergistic cytotoxicity in vitro in FLT3-ITD AML cells, triggering 90% cell death at nanomolar concentrations after 48 hours.

Keywords: dual PI3K/mTOR inhibitors; acute myeloid leukemia (AML); FLT3-ITD; quizartinib; PF-04691502; combination therapy.

Introduction

Acute myeloid leukemia (AML) is an aggressive, heterogeneous clonal disease associated with high mortality (Döhner et al., 2015; Saultz and Garzon, 2016). The backbone of drug treatment relies on chemotherapy and targeted therapy, or very recently on immunotherapy. AML is characterized by chromosomal aberrations (45% patients) as well as mutations in genes such as FLT3, NPM1, DNMT3A, IDH1/ IDH2, N/KRAS, TET and fusion genes (Im et al., 2014; Arber et al., 2016; Follo et al., 2020), leading to clonal proliferation of malignant myeloid progenitors that do not reach terminal differentiation (Gebru and Wang, 2020; Darici et al., 2020; Massett et al., 2021) and impair normal hematopoiesis (Kumar, 2011; Lagunas-Rangel et al., 2017). Like karyotype aberrations, mutations are now recognized as important diagnostic and/or prognostic markers. Notably, some AML recurrent mutations represent ideal druggable targets, and compounds with the desired activity have already reached the clinic. One such target is the class 3 receptor Fms-like tyrosine kinase 3 (FLT3) (Kennedy and Smith, 2020). Following activation by its ligand FLT3, downstream signaling is elicited via the phosphatidylinositol 3-kinase/AKT/mTOR (PI3K/AKT/mTOR) pathway and the Ras/Raf/MEK/ERK pathway (Takahashi, 2011). Mutations at the internal tandem duplication in the juxtamembrane domain coding region (FLT3-ITD), or point mutations of the tyrosine kinase domain (TKD) in FLT3 are the most common alterations in AML, identified in approximately one-third of newly diagnosed adult patients (Stirewalt and Radich, 2003; Papaemmanuil et al., 2016), but common in pediatric AML as well (Bolouri et al., 2018), resulting in ligand-independent activation of the receptor and downstream signaling (Kiyoi et al., 2002).

Regrettably, although a number of small molecules targeting FLT3 have been produced and trialled, the responses in AML patients were only transient while resistance to second-generation inhibitors such as quizartinib occured quite rapidly, thus impairing its clinical impact as monotherapy (Garcia-Horton and Yee, 2020; Smith et al., 2017). Aberrant activation of FLT3, as well as of other oncogenic regulators such as Ras, impact downstream pathways, leading to constitutive PI3K signaling (Bertacchini et al., 2014; Chen et al., 2010). In normal cells activation of class 1A PI3Ks is a tightly

regulated multistep process triggered by binding of the regulatory p85 subunit to phosphorylated growth factor receptors or adaptor proteins in proximity to the plasma membrane (Manning and Toker, 2017; Rathinaswamy and Burke, 2020), where the minor but essential constituent of plasma membranes phosphatidylinositol 4,5-bisphosphate (PIP2) is located (Lo Vasco et al., 2004; Ratti et al., 2021), although its essential nuclear location is also very well described (Maraldi et al., 1993; Follo et al., 2012). Activated PI3K thus converts PIP2 into phosphatidylinositol (3,4,5)-trisphosphate (PIP3) (Manning and Toker, 2017; Hirsch et al., 2020). This way, the signal is relayed to effectors such as AKT and mTOR, and propagates into multiple downstream branches, which undergo complex cross-talk ultimately allowing PI3K to control most cellular activities (Lucarelli et al., 2002; McCubrey et al., 2007; Bulj et al., 2013; Naeem et al., 2015; Hermida et al., 2017; Ruzzene et al., 2017; Bertacchini et al., 2019). Due to its key roles and constitutive activation in most human cancers, a number of compounds targeting the various nodes of the PI3K pathway were developed and subject to extensive screening in vitro and in vivo (Alzahrani, 2019; Hillmann and Fabbro, 2019; Braglia et al., 2020). Unfortunately, most compounds failed in clinical trials, due to intolerable adverse reactions as well as compensatory mechanisms or feedback loops, which reactivate the pathway following chronic inhibition thus hindering treatment efficacy (Alzahrani,2019; Hillmann and Fabbro, 2019).

It has been reported recently that due to long hospitalization and expensive diagnostic testing and therapies, the economic burden of blood disorders has reached the amazing amount of several billion per year in Europe (Luengo-Fernandez et al., 2016) that is expected to increase because of the aging global population and the high cost of novel drug discovery and production. On the other hand, hitherto dozens of selective and powerful drugs have been produced, which have not entered the clinic because of detrimental side effects. However, if administered to the right patient subgroup in combination with other therapeutic agents, such as standard chemotherapy or targeted drugs, some of these compounds might display tolerable toxicity and increased efficacy at lower concentrations.

In our previous work, we demonstrated that vertical inhibition of PI3K and mTOR by NVPBEZ235 showed strong cytotoxicity not only towards AML cell lines, but also in primary blast cells grown in protective conditions such as co-culturing with stroma (Bertacchini et al., 2018). Remarkably, NVPBEZ235 was able to target the CD34+/CD38-/CD123+ cancer stem cell subpopulation in a group of patients. This result deserved further investigation of the efficacy of dual PI3K/mTOR *versus* single PI3K inhibition in AML.

Quite interestingly, it has been shown that aberrant activation of the PI3K/AKT/mTOR pathway promotes resistance to FLT3 inhibition by sorafenib (Lindblad et al., 2016). Moreover, combined inhibition of mTOR and FLT3 showed synergistic cytotoxicity in CML caused by FLT3 mutation (Mohi et al., 2004; Wang et al., 2015). In addition, the anti-diabetic biguanide metformin (Candido et al., 2018), that has been shown to exert anti-cancer effects through the inhibition of the PI3K/mTOR, displayed synergistic effect with sorafenib in FLT3-ITD cell lines (Wang et al., 2015), and a phase I study is ongoing (NCT00819546) with concomitant FLT3 and mTOR inhibition by midostaurin and everolimus respectively.

On this basis, we tested the PI3K/mTOR inhibitors PF-04691502 and LY-3023414 (Bendell et al., 2018; Rubinstein et al., 2020), and compared them to the p110δ isoform-selective inhibitor CAL-101 (idelalisib) (FDA-approved for lymphoid malignancies) (Herman et al., 2010; So and Fruman, 2012; Miller et al., 2015). Although these compounds failed to achieve the expected success in clinical trials as monotherapy, they displayed clinical benefit response in combination therapies (Del Campo et al., 2016; Danilov et al., 2020). Consequently, we assessed their efficacy in association with quizartinib in FLT3-ITD cells compared to AML cells carrying wild-type FLT3.

Materials and methods

CAL-101, LY-3023414 and PF-04691502 were obtained from Selleckchem, and were reconstituted as 10 mM stock solutions in DMSO then stored at -20°C.

Cell lines (THP-1, Kasumi-1, NOMO-1, U937, OCI-AML3, HL60, MOLM-13 and MV4-11) (Table 1) were purchased from DSMZ (Germany) and were cultured in RPMI 1640 medium supplemented with 10% (v/v) fetal bovine serum (FBS) and 2 mM L-glutamine at 37°C, 5% CO2 in a humidified incubator. All cell culture reagents were from Thermo Fisher Scientific. Cells were treated with either vehicle control or increasing concentrations of drugs as indicated. Growth inhibition was assessed by colorimetric resazurin assay (Uzarski et al., 2017) or 3-(4,5-dimethylthiazol-2-yl)-2,5 diphenyl tetrazolium bromide (MTT) assay as described previously (Mediani et al., 2016).

Cell cycle analysis. Cells were washed in PBS and fixed at -20°C in 70% ethanol overnight. Following fixation, cells were washed in PBS then stained with propidium iodide (PI)/ ribonuclease A (RNase A) for 30 minutes in the dark at 37˚C before being analysed using the FACSCantoII flow cytometer (BD Biosciences). Data was acquired using BD FACS Diva software. The percentage of cells in each cell phase: G0/G1, S, or G2M was quantified using FlowJo software.

Apoptosis assay. Cells were washed in Hanks' Balanced Salt Solution (HBSS) and stained with annexin V/DAPI staining (BD Biosciences) for 15 minutes at room temperature in the dark prior to analysis with a flow cytometer as above. The percentage of viable and apoptotic cells was quantified using the FlowJo software.

Combination index (CI) was calculated according to the Chou-Talalay method (Chou and Talalay, 1984) with the CompuSyn software, where CI<1 indicates synergism, CI=1 additive effect, and CI>1 antagonism, whereas CI by Bliss Independence method (Zhao et al., 2014) was calculated using SynergyFinder (version 2.0).

Reverse Phase Protein Array analysis (RPPA). RPPA array assembly, printing, staining and analysis were performed as reported previously (Maraldi et al., 2011; Cimmino et al., 2016; Zampini et al., 2016; Serafin et al., 2017). Briefly, cells were lysed on ice for 30 minutes in TPER Reagent (Pierce,

Rockford, IL), 300 mM NaCl, 1 mM Na Orthovanadate, 200 mM PEFABLOC (AEBSF) (Roche, Basel, Switzerland), 5 μg Aprotinin (Sigma-Aldrich, St Louis, MO, USA), 5μg Pepstatin A (Sigma-Aldrich, St Louis, MO, USA), 5μg Leupeptin (Sigma-Aldrich, St Louis, MO, USA). All samples were diluted to a final concentration of 0.5 mg/mL with Tris-Glycine SDS buffer + β-mercaptoethanol and then 30 μL of each sample were loaded on a 384-well plate in a series of 4-fold dilutions and printed in duplicate on nitrocellulose coated glass slides (ONCYTE Nitrocellulose Film Slides, Grace Bio-Labs, Oregon, USA). Then, the slides were subjected to immunostaining with the indicated antibodies. Slides were stained on an automated slide stainer (Dako, Carpinteria, CA, U.S.A) using a biotin-linked peroxidase catalyzed signal amplification. Both primary and secondary antibodies were obtained from Cell Signaling Technology and had been validated previously (Maraldi et al., 2011; Serafin et al., 2017).

Statistical analysis. The data is either shown as individual values or as an average. Error bars represent the standard deviation (SD). Statistical analysis was performed using the GraphPad Prism software. To compare two groups, paired student's t-test was performed and to compare multiple groups, paired one-way ANOVA with multiple comparisons test was performed. A p-value of <0.05 was considered significant.

Results and Discussion.

AML cell lines display differential sensitivity to PI3K signaling blockade

Here we explored whether PI3K oncogenic signaling downstream of the most common AML phenotypes such as mutant Ras or FLT3 can be disrupted by blocking PI3K or by dual inhibition of PI3K/mTOR. Thus, we screened the ATP-competitive PI3K/mTOR inhibitors PF-04691502 and LY-3023414, and the p110δ-selective PI3K inhibitor CAL-101 in a panel of cell lines carrying the most frequently described mutations in AML patients (Table 1).

Contrary to previous reports (Nguyen, et al., 2014), our results clearly show that all cell lines tested were resistant to inhibition of p110δ by CAL-101 even at the highest concentration (4 μM), in terms of cell viability (Figure 1A and Figure 1S). Conversely, PI3K/mTOR inactivation by LY-3023414 or PF-04691502 resulted in a clear-cut concentration- and time-dependent decrease ($p>0,0001$) in all cell lines except the NPM1 and R882C-DNMT3A mutant OCI-AML3 cells (Martelli et al., 2010) (Figure 1B-C and Figure 1S). It is worth noting that FLT3-ITD cells displayed a remarkably high sensitivity towards PI3K/mTOR signaling inhibition at concentrations close to the IC50 range (a selection is shown in Table 1S).

Dual PI3K/mTOR targeting triggers caspase 7 and PARP cleavage in FLT3-ITD cells

Next, the ability of these drugs to induce apoptosis was monitored through cleavage of well-known apoptotic markers, namely the effector caspase 7 and its target poly(ADP ribose) polymerase 1 (PARP) (Tewari et al., 1995) by RPPA analysis. Cell lines exhibited very different behaviors in response to drug treatment (Figure 2). In particular, MOLM-13 and MV4-11 were remarkably sensitive to targeted signaling blockade, especially by PF-04691502 (Figure 2B). NOMO-1, Kasumi-1 and U937 cells displayed a significant increase of active caspase 7, although the timing of the response was cell line dependent, being between 16 and 48 hours (Figure 2S). Quite unexpectedly, OCI-AML3 cells showed some degree of PARP inhibition too, whereas HL60 were resistant to

treatment, as very low levels of cleaved caspase 7 or PARP were detectable up to 48 hours. Thus in this first part of our work we established that AML cell lines carrying the FLT3-ITD mutation showed high sensitivity to dual inhibition of PI3K/mTOR both in terms of reduction of cell viability and cleavage of apoptosis markers.

PI3K/mTOR inhibition robustly abrogates signaling in FLT3-ITD cells

We then asked whether the effect on cell viability was mirrored by inhibition of signaling by the same compounds, i.e., if the sensitivity of FLT3-ITD AML cell lines to drugs targeting the PI3K pathway correlated with their ability to abrogate phosphorylation of key endpoints durably, thus avoiding rebound signaling. As a readout of PI3K and mTOR inhibition, we therefore monitored phosphorylation of AKT (Manning and Toker, 2017), GSK3 (Evangelisti et al, 2020; McCubrey et al., 2016; Steelman et al., 2016) and S6 ribosomal protein (S6RP) (Ruvinsky and Meyuhas, 2006) through RPPA analysis. In line with our aforementioned observations, PF-04691502 and LY-3023414 were able to evoke a dramatic, long-lasting reduction in phosphorylation of the selected epitopes in MOLM-13 and MV4-11, whereas response to CAL-101 was very poor (Figure 3). In contrast, HL-60, NOMO-1 and Kasumi cells showed no or very low sensitivity to these compounds even upon pulse treatment (1 hour) (Figure 3S). On the other hand, an early reduction of phosphorylation was clearly detectable in U937, OCI-AML3 and THP-1. With the exception of THP-1 cells, signaling inhibition did not last, though, and AKT activity recovered quickly (Figure 3S).

Dual PI3K/mTOR inhibitors display synergistic cytotoxicity with quizartinib in FLT3-ITD cells

We have shown that the cytotoxic response and the apoptotic markers of different cell lines, as well as PI3K pathway activation profiling, indicate that FLT3-ITD cells are better responders to PI3K/mTOR signaling inhibition than other AML common phenotypes such as NPM1 mutant cells. Therefore, next we explored whether the association with the selective FLT3 inhibitor quizartinib potentiated the ability of PF-04691502 to kill FLT3-ITD AML cells.

First, we compared the efficacy of PF-04691502 alongside the selective FLT3 inhibitor quizartinib in FLT3-ITD MOLM-13 and MV4-11 *versus* wild-type FLT3 THP-1 cells (Figure 4A). Indeed, in a time course resazurin-based cell viability assay, both PF-04691502 and quizartinib potently decreased the viability of both MOLM-13 (IC50 160.9 nM and 0.7 nM, respectively) and MV4-11 (IC50 195.4 nM and 0.6 nM, respectively) (Table 1S). Importantly, the observed effect for quizartinib was selective for FLT3-ITD cells as quizartinib did not reduce the viability of wild-type FLT3 THP-1 cells (Figure 4A). We further investigated whether the observed reduction of viability was caused by cell cycle arrest and/or death via apoptosis. Accordingly, a parallel increase of cells arrested in G1 phase was detectable after 24 hours treatment (Figure 4B), together with a significant, though not dramatic, increase of apoptosis, particularly after 48 hours, only in MOLM-13 and MV4-11 cells (Figure 4C). FLT3 wild-type cell line THP-1 was also treated with quizartinib to exclude off-target effects (Figure 4B-C).

Furthermore, we evaluated the efficacy of MOLM-13 cells exposed to a concentration range of quizartinib and PF-04691502 around their respective IC50s, for 48 hours, either alone or in combination. Remarkably, we observed that concomitant addition to the culture medium of PF-04691502 and quizartinib at concentrations as low as 120 nM PF-04691502 and 1.44 nM quizartinib exerted enhanced reduction of viability and this effect was found to be synergistic (Combination Index score of 0.4) (Figure 5A). In addition, assessing cell cycle status and apoptosis revealed enhanced G1 phase arrest, and more than double the number of apoptotic cells with respect to single-agent treatment, reaching 90% cell death at 240 and 2.88 nM PF-04691502 and quizartinib respectively (Figure 5B-C). This data represents the first report of a potent synergistic antileukemic effect upon concomitant targeting of FLT3 and PI3K/mTOR in FLT3-ITD AML cells.

Twenty years on from the FDA approval of the first kinase inhibitor, imatinib, for the treatment of CML (Cohen et al., 2002), targeted inhibition of oncogenic signaling is regarded as a central option for modern oncology. Pharmaceutical companies and the scientific community are fully committed to the development of selective inhibitors of oncogenes such as PI3K or FLT3 kinases and many

selective and potent compounds have been identified. With few exceptions, however, despite extraordinary costs and efforts, most compounds give rise to primary or secondary resistance (Alzahrani, 2019; Hillmann and Fabbro, 2019) underlining that more cost-effective strategies are urgently required. Promising results may come from current trials where PI3K/mTOR inhibitors, already marketed but not in clinical use because of modest effect or long-term adverse events as single agents, are combined to achieve parallel pathways inhibition, targeted and non-targeted combinations or with other antitumor agents (Darici et al., 2020; Alzahrani, 2019; Herschbein and Liesveld, 2018; Grignani et al., 2015). This strategy would have significant advantages, as all the important characteristics of these drugs, such as their pharmacokinetics, pharmacodynamics and toxicity have already undergone extensive study not only in cell and animal models but also in patients. Consistent with this line of evidence, our work, although performed only in cell lines in vitro, highlighted that in FLT3-ITD AML cells the combination with FLT3 inhibitors could unlock the potential of PI3K/mTOR blocking compounds that did not reach the clinic, such as PF-04691502, leading to synergistic cytotoxicity at much lower concentrations than single-agent therapy.

Acknowledgments

This research was supported by grants from the not-for-profit Associazione Mantovana per la Ricerca sul Cancro (A.Ma.Ri.Ca); V.S has received funding from Fondazione Associazione Italiana per la Ricerca sul Cancro (AIRC) under MFAG 2018 - ID. 21771.

References

Alzahrani, A.S., 2019. PI3K/Akt/mTOR inhibitors in cancer: At the bench and bedside. Semin Cancer Biol 59, 125–132. https://doi.org/10.1016/j.semcancer.2019.07.009

Arber, D.A., Orazi, A., Hasserjian, R., Thiele, J., Borowitz, M.J., Le Beau, M.M., Bloomfield, C.D., Cazzola, M., Vardiman, J.W., 2016. The 2016 revision to the World Health Organization classification of myeloid neoplasms and acute leukemia. Blood 127, 2391–2405. https://doi.org/10.1182/blood-2016-03-643544

Bendell, J.C., Varghese, A.M., Hyman, D.M., Bauer, T.M., Pant, S., Callies, S., Lin, J., Martinez, R., Wickremsinhe, E., Fink, A., Wacheck, V., Moore, K.N., 2018. A First-in-Human Phase 1 Study of LY3023414, an Oral PI3K/mTOR Dual Inhibitor, in Patients with Advanced Cancer. Clin Cancer Res 24, 3253–3262. https://doi.org/10.1158/1078-0432.CCR-17-3421

Bertacchini J, Mediani L, Beretti F, Guida M, Ghalali A, Brugnoli F, Bertagnolo V, Petricoin E, Poti F, Arioli J, Anselmi L, Bari A, McCubrey J, Martelli AM, Cocco L, Capitani S, Marmiroli S. 2019. Clusterin enhances AKT2-mediated motility of normal and cancer prostate cells through a PTEN and PHLPP1 circuit. J Cell Physiol. 234, 11188-11199. https://doi.org/10.1002/jcp.27768.

Bertacchini, J., Frasson, C., Chiarini, F., D'Avella, D., Accordi, B., Anselmi, L., Barozzi, P., Forghieri, F., Luppi, M., Martelli, A.M., Basso, G., Najmaldin, S., Khosravi, A., Rahim, F., Marmiroli, S., 2018. Dual inhibition of PI3K/mTOR signaling in chemoresistant AML primary cells. Adv Biol Regul. 68, 2–9. https://doi.org/10.1016/j.jbior.2018.03.001

Bertacchini, J., Guida, M., Accordi, B., Mediani, L., Martelli, A.M., Barozzi, P., Petricoin, E., Liotta, L., Milani, G., Giordan, M., Luppi, M., Forghieri, F., De Pol, A., Cocco, L., Basso, G., Marmiroli, S., 2014. Feedbacks and adaptive capabilities of the PI3K/Akt/mTOR axis in

acute myeloid leukemia revealed by pathway selective inhibition and phosphoproteome analysis. Leukemia 28, 2197–2205. https://doi.org/10.1038/leu.2014.123

Bolouri, H., Farrar, J.E., Triche, T., Ries, R.E., Lim, E.L., Alonzo, T.A., Ma, Y., Moore, R., Mungall, A.J., Marra, M.A., Zhang, J., Ma, X., Liu, Yu, Liu, Yanling, Auvil, J.M.G., Davidsen, T.M., Gesuwan, P., Hermida, L.C., Salhia, B., Capone, S., Ramsingh, G., Zwaan, C.M., Noort, S., Piccolo, S.R., Kolb, E.A., Gamis, A.S., Smith, M.A., Gerhard, D.S., Meshinchi, S., 2018. The molecular landscape of pediatric acute myeloid leukemia reveals recurrent structural alterations and age-specific mutational interactions. Nat Med 24, 103–112. https://doi.org/10.1038/nm.4439

Braglia, L., Zavatti, M., Vinceti, M., Martelli, A.M., Marmiroli, S., 2020. Deregulated PTEN/PI3K/AKT/mTOR signaling in prostate cancer: Still a potential druggable target? Biochim Biophys Acta Mol Cell Res 1867, 118731. https://doi.org/10.1016/j.bbamcr.2020.118731

Bulj Z, Duchi S, Bevilacqua A, Gherardi A, Dozza B, Piccinini F, Adalgisa Mariani G, Lucarelli E, Giannini S, Donati D, Marmiroli S, 2013. Protein kinase B/AKT isoform 2 drives migration of human mesenchymal stem cells. Int J Oncol. 42,118-26. https://doi.org/10.3892/ijo.2012.1700

Candido, S., Abrams, S.L., Steelman, L., Lertpiriyapong, K., Martelli, A.M., Cocco, L., Ratti, S., Follo, M.Y., Murata, R.M., Rosalen, P.L., Lombardi, P., Montalto, G., Cervello, M., Gizak, A., Rakus, D., Suh, P.-G., Libra, M., McCubrey, J.A., 2018. Metformin influences drug sensitivity in pancreatic cancer cells. Adv Biol Regul 68, 13–30. https://doi.org/10.1016/j.jbior.2018.02.002

Chen, W., Drakos, E., Grammatikakis, I., Schlette, E.J., Li, J., Leventaki, V., Staikou-Drakopoulou, E., Patsouris, E., Panayiotidis, P., Medeiros, L.J., Rassidakis, G.Z., 2010. mTOR signaling is

activated by FLT3 kinase and promotes survival of FLT3-mutated acute myeloid leukemia cells. Mol Cancer 9, 292. https://doi.org/10.1186/1476-4598-9-292

Chou TC, Talalay P. 1984 Quantitative analysis of dose-effect relationships: the combined effects of multiple drugs or enzyme inhibitors. Adv Enzyme Regul; 22:27-55. https://doi.org/10.1016/0065-2571(84)90007-4.

Cohen, M.H., Williams, G., Johnson, J.R., Duan, J., Gobburu, J., Rahman, A., Benson, K., Leighton, J., Kim, S.K., Wood, R., Rothmann, M., Chen, G., U, K.M., Staten, A.M., Pazdur, R., 2002. Approval summary for imatinib mesylate capsules in the treatment of chronic myelogenous leukemia. Clin Cancer Res 8, 935–942.

Cimmino, F., Pezone, L., Avitabile, M., Persano, L., Vitale, M., Sassi, M., Bresolin, S., Serafin, V., Zambrano, N., Scaloni, A., Basso, G., Iolascon, A., Capasso, M., 2016 Proteomic Alterations in Response to Hypoxia Inducible Factor 2α in Normoxic Neuroblastoma Cells. J Proteome Res. 7;15(10):3643-3655. doi: 10.1021/acs.jproteome.6b00457.

Danilov, A.V., Herbaux, C., Walter, H.S., Hillmen, P., Rule, S.A., Kio, E.A., Karlin, L., Dyer, M.J.S., Mitra, S.S., Yi, P.C., Humeniuk, R., Huang, X., Zhou, Z., Bhargava, P., Jürgensmeier, J.M., Fegan, C.D., 2020. Phase Ib Study of Tirabrutinib in Combination with Idelalisib or Entospletinib in Previously Treated Chronic Lymphocytic Leukemia. Clin Cancer Res 26, 2810–2818. https://doi.org/10.1158/1078-0432.CCR-19-3504

Darici, S., Alkhaldi, H., Horne, G., Jørgensen, H.G., Marmiroli, S., Huang, X., 2020. Targeting PI3K/Akt/mTOR in AML: Rationale and Clinical Evidence. Journal of Clinical Medicine 9, 2934. https://doi.org/10.3390/jcm9092934

Del Campo, J.M., Birrer, M., Davis, C., Fujiwara, K., Gollerkeri, A., Gore, M., Houk, B., Lau, S., Poveda, A., González-Martín, A., Muller, C., Muro, K., Pierce, K., Suzuki, M., Vermette, J., Oza, A., 2016. A randomized phase II non-comparative study of PF-04691502 and

gedatolisib (PF-05212384) in patients with recurrent endometrial cancer. Gynecol. Oncol. 142, 62–69. https://doi.org/10.1016/j.ygyno.2016.04.019

Döhner, H., Weisdorf, D.J., Bloomfield, C.D., 2015. Acute Myeloid Leukemia. N Engl J Med 373, 1136–1152. https://doi.org/10.1056/NEJMra1406184

Evangelisti, C., Chiarini, F., Paganelli, F., Marmiroli, S., Martelli, A.M., 2020. Crosstalks of GSK3 signaling with the mTOR network and effects on targeted therapy of cancer. Biochim Biophys Acta Mol Cell Res 1867, 118635. https://doi.org/10.1016/j.bbamcr.2019.118635

Follo, M.Y., Pellagatti, A., Ratti, S., Ramazzotti, G., Faenza, I., Fiume, R., Mongiorgi, S., Suh, P.-G., McCubrey, J.A., Manzoli, L., Boultwood, J., Cocco, L., 2020. Recent advances in MDS mutation landscape: Splicing and signalling. Adv Biol Regul 75, 100673. https://doi.org/10.1016/j.jbior.2019.100673

Follo MY, Mongiorgi S, Clissa C, Paolini S, Martinelli G, Martelli AM, Fioravanti G, Manzoli L, Finelli C, Cocco L., 2012 Activation of nuclear inositide signalling pathways during erythropoietin therapy in low-risk MDS patients. Leukemia 26(12):2474-82 https://doi.org/10.1038/leu.2012.133

Garcia-Horton, A., Yee, K.W., 2020. Quizartinib for the treatment of acute myeloid leukemia. Expert Opin Pharmacother 21, 2077–2090. https://doi.org/10.1080/14656566.2020.1801637

Gebru, M.T., Wang, H.-G., 2020. Therapeutic targeting of FLT3 and associated drug resistance in acute myeloid leukemia. Journal of Hematology & Oncology 13, 155. https://doi.org/10.1186/s13045-020-00992-1

Grignani, G., Palmerini, E., Ferraresi, V., D'Ambrosio, L., Bertulli, R., Asaftei, S.D., Tamburini, A., Pignochino, Y., Sangiolo, D., Marchesi, E., Capozzi, F., Biagini, R., Gambarotti, M., Fagioli, F., Casali, P.G., Picci, P., Ferrari, S., Aglietta, M., Italian Sarcoma Group, 2015. Sorafenib and everolimus for patients with unresectable high-grade osteosarcoma

progressing after standard treatment: a non-randomised phase 2 clinical trial. Lancet Oncol. 16, 98–107. https://doi.org/10.1016/S1470-2045(14)71136-2

Herman, S.E.M., Gordon, A.L., Wagner, A.J., Heerema, N.A., Zhao, W., Flynn, J.M., Jones, J., Andritsos, L., Puri, K.D., Lannutti, B.J., Giese, N.A., Zhang, X., Wei, L., Byrd, J.C., Johnson, A.J., 2010. Phosphatidylinositol 3-kinase-δ inhibitor CAL-101 shows promising preclinical activity in chronic lymphocytic leukemia by antagonizing intrinsic and extrinsic cellular survival signals. Blood 116, 2078–2088. https://doi.org/10.1182/blood-2010-02-271171

Hermida, M.A., Dinesh Kumar, J., Leslie, N.R., 2017. GSK3 and its interactions with the PI3K/AKT/mTOR signalling network. Adv Biol Regul 65, 5–15. https://doi.org/10.1016/j.jbior.2017.06.003

Herschbein, L., Liesveld, J.L., 2018. Dueling for dual inhibition: Means to enhance effectiveness of PI3K/Akt/mTOR inhibitors in AML. Blood Rev. 32, 235–248. https://doi.org/10.1016/j.blre.2017.11.006

Hillmann, P., Fabbro, D., 2019. PI3K/mTOR Pathway Inhibition: Opportunities in Oncology and Rare Genetic Diseases. Int J Mol Sci. 20. https://doi.org/10.3390/ijms20225792

Hirsch E, Gulluni F, Martini M. Phosphoinositides in cell proliferation and metabolism. Adv Biol Regul. 2020 Jan;75:100693. doi: 10.1016/j.jbior.2020.100693.

Im, A.P., Sehgal, A.R., Carroll, M.P., Smith, B.D., Tefferi, A., Johnson, D.E., Boyiadzis, M., 2014. DNMT3A and IDH mutations in acute myeloid leukemia and other myeloid malignancies: associations with prognosis and potential treatment strategies. Leukemia 28, 1774–1783. https://doi.org/10.1038/leu.2014.124

Kennedy, V.E., Smith, C.C., 2020. FLT3 Mutations in Acute Myeloid Leukemia: Key Concepts and Emerging Controversies. Front Oncol 10, 612880. https://doi.org/10.3389/fonc.2020.612880

Kiyoi, H., Ohno, R., Ueda, R., Saito, H., Naoe, T., 2002. Mechanism of constitutive activation of FLT3 with internal tandem duplication in the juxtamembrane domain. Oncogene 21, 2555–2563. https://doi.org/10.1038/sj.onc.1205332

Kumar, C.C., 2011. Genetic abnormalities and challenges in the treatment of acute myeloid leukemia. Genes Cancer 2, 95–107. https://doi.org/10.1177/1947601911408076

Lagunas-Rangel, F.A., Chávez-Valencia, V., Gómez-Guijosa, M.Á., Cortes-Penagos, C., 2017. Acute Myeloid Leukemia-Genetic Alterations and Their Clinical Prognosis. Int J Hematol Oncol Stem Cell Res 11, 328–339.

Lindblad, O., Cordero, E., Puissant, A., Macaulay, L., Ramos, A., Kabir, N.N., Sun, J., Vallon-Christersson, J., Haraldsson, K., Hemann, M.T., Borg, Å., Levander, F., Stegmaier, K., Pietras, K., Rönnstrand, L., Kazi, J.U., 2016. Aberrant activation of the PI3K/mTOR pathway promotes resistance to sorafenib in AML. Oncogene 35, 5119–5131. https://doi.org/10.1038/onc.2016.41

Lo Vasco VR, Calabrese G, Manzoli L, Palka G, Spadano A, Morizio E, Guanciali-Franchi P, Fantasia D, Cocco L., 2004 Inositide-specific phospholipase c beta1 gene deletion in the progression of myelodysplastic syndrome to acute myeloid leukemia. Leukemia. 18(6):1122-6. https://doi.org/10.1038/sj.leu.2403368.

Lucarelli E, Sangiorgi L, Maini V, Lattanzi G, Marmiroli S, Reggiani M, Mordenti M, Alessandra Gobbi G, Scrimieri F, Zambon Bertoja A, Picci P., 2002. Troglitazione affects survival of human osteosarcoma cells. Int J Cancer. 98(3):344-51. https://doi.org/10.1002/ijc.10203.

Luengo-Fernandez, R., Burns, R., Leal, J., 2016. Economic burden of non-malignant blood disorders across Europe: a population-based cost study. Lancet Haematol 3, e371-378. https://doi.org/10.1016/S2352-3026(16)30061-8

Manning, B.D., Toker, A., 2017. AKT/PKB Signaling: Navigating the Network. Cell 169, 381–405. https://doi.org/10.1016/j.cell.2017.04.001

Maraldi, N.M., Zini, N., Santi, S., Bavelloni, A., Valmori, A., Marmiroli, S., Ognibene, A., 1993. Phosphoinositidase C isozymes in SaOS-2 cells: immunocytochemical detection in nuclear and cytoplasmic compartments. Biol Cell 79, 243–250. https://doi.org/10.1016/0248-4900(93)90143-3

Maraldi, T., Bertacchini, J., Benincasa, M., Guida, M., De Pol, A., Liotta, L.A., Petricoin, E., Cocco, L., Marmiroli, S., 2011. Reverse-phase protein microarrays (RPPA) as a diagnostic and therapeutic guide in multidrug resistant leukemia. Int J Oncol 38, 427–435. https://doi.org/10.3892/ijo.2010.850

Martelli, M.P., Pettirossi, V., Thiede, C., Bonifacio, E., Mezzasoma, F., Cecchini, D., Pacini, R., Tabarrini, A., Ciurnelli, R., Gionfriddo, I., Manes, N., Rossi, R., Giunchi, L., Oelschlägel, U., Brunetti, L., Gemei, M., Delia, M., Specchia, G., Liso, A., Di Ianni, M., Di Raimondo, F., Falzetti, F., Del Vecchio, L., Martelli, M.F., Falini, B., 2010. CD34+ cells from AML with mutated NPM1 harbor cytoplasmic mutated nucleophosmin and generate leukemia in immunocompromised mice. Blood 116, 3907–3922. https://doi.org/10.1182/blood-2009-08-238899

Massett, M.E., Monaghan, L., Patterson, S., Mannion, N., Bunschoten, R.P., Hoose, A., Marmiroli, S., Liskamp, R.M.J., Jørgensen, H.G., Vetrie, D., Michie, A.M., Huang, X., 2021. A KDM4A-PAF1-mediated epigenomic network is essential for acute myeloid leukemia cell

self-renewal and survival. Cell Death Dis 12, 1–16. https://doi.org/10.1038/s41419-021-03738-0

McCubrey, J.A., Rakus, D., Gizak, A., Steelman, L.S., Abrams, S.L., Lertpiriyapong, K., Fitzgerald, T.L., Yang, L.V., Montalto, G., Cervello, M., Libra, M., Nicoletti, F., Scalisi, A., Torino, F., Fenga, C., Neri, L.M., Marmiroli, S., Cocco, L., Martelli, A.M., 2016. Effects of mutations in Wnt/β-catenin, hedgehog, Notch and PI3K pathways on GSK-3 activity-Diverse effects on cell growth, metabolism and cancer. Biochim. Biophys. Acta 1863, 2942–2976. https://doi.org/10.1016/j.bbamcr.2016.09.004

McCubrey, J.A., Steelman, L.S., Chappell, W.H., Abrams, S.L., Wong, E.W.T., Chang, F., Lehmann, B., Terrian, D.M., Milella, M., Tafuri, A., Stivala, F., Libra, M., Basecke, J., Evangelisti, C., Martelli, A.M., Franklin, R.A., 2007. Roles of the Raf/MEK/ERK pathway in cell growth, malignant transformation and drug resistance. Biochim Biophys Acta 1773, 1263–1284. https://doi.org/10.1016/j.bbamcr.2006.10.001

Mediani, L., Gibellini, F., Bertacchini, J., Frasson, C., Bosco, R., Accordi, B., Basso, G., Bonora, M., Calabrò, M.L., Mattiolo, A., Sgarbi, G., Baracca, A., Pinton, P., Riva, G., Rampazzo, E., Petrizza, L., Prodi, L., Milani, D., Luppi, M., Potenza, L., De Pol, A., Cocco, L., Capitani, S., Marmiroli, S., 2016. Reversal of the glycolytic phenotype of primary effusion lymphoma cells by combined targeting of cellular metabolism and PI3K/Akt/ mTOR signaling. Oncotarget 7, 5521–5537. https://doi.org/10.18632/oncotarget.6315

Miller, B.W., Przepiorka, D., de Claro, R.A., Lee, K., Nie, L., Simpson, N., Gudi, R., Saber, H., Shord, S., Bullock, J., Marathe, D., Mehrotra, N., Hsieh, L.S., Ghosh, D., Brown, J., Kane, R.C., Justice, R., Kaminskas, E., Farrell, A.T., Pazdur, R., 2015. FDA approval: idelalisib monotherapy for the treatment of patients with follicular lymphoma and small lymphocytic lymphoma. Clin. Cancer Res. 21, 1525–1529. https://doi.org/10.1158/1078-0432.CCR-14-2522

Mohi, M.G., Boulton, C., Gu, T.-L., Sternberg, D.W., Neuberg, D., Griffin, J.D., Gilliland, D.G., Neel, B.G., 2004. Combination of rapamycin and protein tyrosine kinase (PTK) inhibitors for the treatment of leukemias caused by oncogenic PTKs. Proc Natl Acad Sci U S A 101, 3130–3135. https://doi.org/10.1073/pnas.0400063101

Naeem AS, Zhu Y, Di WL, Marmiroli S, O'Shaughnessy RF, 2015. AKT1-mediated Lamin A/C degradation is required for nuclear degradation and normal epidermal terminal differentiation. Cell Death Differ. 22, 2123-32. doi: 10.1038/cdd.2015.62.

Nguyen, L.X.T., Sesay, A., Mitchell, B.S., 2014. Effect of CAL-101, a PI3Kδ inhibitor, on ribosomal rna synthesis and cell proliferation in acute myeloid leukemia cells. Blood Cancer J. 4, e228. https://doi.org/10.1038/bcj.2014.49

Papaemmanuil, E., Gerstung, M., Bullinger, L., Gaidzik, V.I., Paschka, P., Roberts, N.D., Potter, N.E., Heuser, M., Thol, F., Bolli, N., Gundem, G., Van Loo, P., Martincorena, I., Ganly, P., Mudie, L., McLaren, S., O'Meara, S., Raine, K., Jones, D.R., Teague, J.W., Butler, A.P., Greaves, M.F., Ganser, A., Döhner, K., Schlenk, R.F., Döhner, H., Campbell, P.J., 2016. Genomic Classification and Prognosis in Acute Myeloid Leukemia. N Engl J Med 374, 2209–2221. https://doi.org/10.1056/NEJMoa1516192

Rathinaswamy, M.K., Burke, J.E., 2020. Class I phosphoinositide 3-kinase (PI3K) regulatory subunits and their roles in signaling and disease. Adv Biol Regul 75, 100657. https://doi.org/10.1016/j.jbior.2019.100657

Ratti, S., Evangelisti, C., Mongiorgi, S., De Stefano, A., Fazio, A., Bonomini, F., Follo, M.Y., Faenza, I., Manzoli, L., Sheth, B., Vidalle, M.C., Kimber, S.T., Divecha, N., Cocco, L., Fiume, R., 2021. Modulating Phosphoinositide Profiles as a Roadmap for Treatment in Acute Myeloid Leukemia. Front Oncol 11, 678824. https://doi.org/10.3389/fonc.2021.678824

Rubinstein, M.M., Hyman, D.M., Caird, I., Won, H., Soldan, K., Seier, K., Iasonos, A., Tew, W.P., O'Cearbhaill, R.E., Grisham, R.N., Hensley, M.L., Troso-Sandoval, T., Sabbatini, P., Guillen, J., Selcuklu, S.D., Zimel, C., Torrisi, J., Aghajanian, C., Makker, V., 2020. Phase 2 study of LY3023414 in patients with advanced endometrial cancer harboring activating mutations in the PI3K pathway. Cancer 126, 1274–1282. https://doi.org/10.1002/cncr.32677

Ruvinsky, I., Meyuhas, O., 2006. Ribosomal protein S6 phosphorylation: from protein synthesis to cell size. Trends Biochem. Sci. 31, 342–348. https://doi.org/10.1016/j.tibs.2006.04.003

Ruzzene, M., Bertacchini, J., Toker, A., Marmiroli, S., 2017. Cross-talk between the CK2 and AKT signaling pathways in cancer. Adv Biol Regul 64, 1–8. https://doi.org/10.1016/j.jbior.2017.03.002

Saultz, J.N., Garzon, R., 2016. Acute Myeloid Leukemia: A Concise Review. J Clin Med. 5. https://doi.org/10.3390/jcm5030033

Serafin, V., Lissandron, V., Buldini, B., Bresolin, S., Paganin, M., Grillo, F., Andriano, N., Palmi, C., Cazzaniga, G., Marmiroli, S., Conter, V., Basso, G., Accordi, B., 2017. Phosphoproteomic analysis reveals hyperactivation of mTOR/STAT3 and LCK/Calcineurin axes in pediatric early T-cell precursor ALL. Leukemia 31, 1007–1011. https://doi.org/10.1038/leu.2017.13

Smith, C.C., Paguirigan, A., Jeschke, G.R., Lin, K.C., Massi, E., Tarver, T., Chin, C.-S., Asthana, S., Olshen, A., Travers, K.J., Wang, S., Levis, M.J., Perl, A.E., Radich, J.P., Shah, N.P., 2017. Heterogeneous resistance to quizartinib in acute myeloid leukemia revealed by single-cell analysis. Blood 130, 48–58. https://doi.org/10.1182/blood-2016-04-711820

So, L., Fruman, D.A., 2012. PI3K signalling in B- and T-lymphocytes: new developments and therapeutic advances. Biochem J 442, 465–481. https://doi.org/10.1042/BJ20112092

Steelman, L.S., Fitzgerald, T., Lertpiriyapong, K., Cocco, L., Follo, M.Y., Martelli, A.M., Neri, L.M., Marmiroli, S., Libra, M., Candido, S., Nicoletti, F., Scalisi, A., Fenga, C., Drobot, L., Rakus, D., Gizak, A., Laidler, P., Dulinska-Litewka, J., Basecke, J., Mijatovic, S., Maksimovic-Ivanic, D., Montalto, G., Cervello, M., Milella, M., Tafuri, A., Demidenko, Z., Abrams, S.L., McCubrey, J.A., 2016. Critical Roles of EGFR Family Members in Breast Cancer and Breast Cancer Stem Cells: Targets for Therapy. Curr Pharm Des 22, 2358–2388. https://doi.org/10.2174/1381612822666160304151011

Stirewalt, D.L., Radich, J.P., 2003. The role of FLT3 in haematopoietic malignancies. Nat Rev Cancer 3, 650–665. https://doi.org/10.1038/nrc1169

Takahashi, S., 2011. Downstream molecular pathways of FLT3 in the pathogenesis of acute myeloid leukemia: biology and therapeutic implications. J Hematol Oncol. 4, 13. https://doi.org/10.1186/1756-8722-4-13

Tewari, M., Quan, L.T., O'Rourke, K., Desnoyers, S., Zeng, Z., Beidler, D.R., Poirier, G.G., Salvesen, G.S., Dixit, V.M., 1995. Yama/CPP32 beta, a mammalian homolog of CED-3, is a CrmA-inhibitable protease that cleaves the death substrate poly(ADP-ribose) polymerase. Cell 81, 801–809. https://doi.org/10.1016/0092-8674(95)90541-3

Uzarski, J.S., DiVito, M.D., Wertheim, J.A., Miller, W.M., 2017. Essential design considerations for the resazurin reduction assay to noninvasively quantify cell expansion within perfused extracellular matrix scaffolds. Biomaterials 129, 163–175. https://doi.org/10.1016/j.biomaterials.2017.02.015

Wang, F., Liu, Z., Zeng, J., Zhu, H., Li, J., Cheng, X., Jiang, T., Zhang, L., Zhang, C., Chen, T., Liu, T., Jia, Y., 2015. Metformin synergistically sensitizes FLT3-ITD-positive acute myeloid leukemia to sorafenib by promoting mTOR-mediated apoptosis and autophagy. Leuk Res 39, 1421–1427. https://doi.org/10.1016/j.leukres.2015.09.016

Zampini, M., Tregnago, C., Bisio, V., Accordi, B., Serafin, V., Pierani, P., Santoro, N., Zecca, M., Micalizzi, C., Putti, M.C., Locatelli, F., Basso, G., Pigazzi, M., 2016. Dna Methylation Is Linked to a Specific Cell-Adhesion Program in Relapsed Pediatric t(8;21)(q22;q22)RUNX1-RUNX1T1 Patients. Blood 128, 1524. https://doi.org/10.1182/blood.V128.22.1524.1524

Zhao, W., Sachsenmeier, K., Zhang, L., Sult, E., Hollingsworth, R.E., Yang, H., 2014. A New Bliss Independence Model to Analyze Drug Combination Data. J Biomol Screen 19, 817–821. https://doi.org/10.1177/1087057114521867

Legends to Figures and Tables.

Table 1. Mutational background of AML cell lines

The mutational background of the cell lines employed in this work is shown.

Figure 1. **AML cell lines display differential sensitivity to PI3K signaling blockade.**

Effect of the addition of increasing concentration of A) CAL-101, B) LY-3023414 and C) PF-04691502 for 24 (left panel) or 48 hours (right panel) on AML cell viability. Values in the heatmap represent the average of three technical triplicates.

Figure 2. Dual inhibition of PI3K/mTOR elicits cleavage of caspase 7 and PARP in FLT3-ITD AML cells.

The status of the apoptosis markers caspase 7 (upper panel) and PARP (lower panel) in MOLM-13 and MV4-11 FLT3-ITD AML cells treated with either PI3K-p110δ or dual PI3K/mTOR inhibitors LY-3023414 and PF-04691502, at the indicated concentrations, was analyzed by RPPA. Control samples, treated with drug vehicle only (DMSO), were included at each time point The results are presented as drug-treated *versus* vehicle-treated cells (%) and are individual values from four replicates showing <5% deviation.

Figure 3 PI3K/mTOR pathway activation in FLT3-ITD AML cells.

Inhibition of PI3K signaling by either the PI3K-p110δ inhibitor CAL-101 or the dual PI3K/mTOR inhibitors LY-3023414 and PF-04691502 was analyzed through RPPA, by comparison of the phosphorylation status of AKT S473, S6RP S240/244, GSK3 S21/3 in MOLM-13 and MV4-11 FLT3-ITD AML cells. The experimental design included three time points, i.e. 1, 16 and 48 hours. Control cells treated with drug vehicle only (DMSO), were included at each time point. The results

are presented as drug-treated *versus* vehicle-treated cells (%) and are individual values from four replicates showing <5% deviation.

Figure 4. PF-04691502 evokes reduction of cell viability, G1 cell cycle arrest and apoptosis in FLT3-ITD AML cells.

THP-1, MOLM-13 and MV4-11 cells were exposed to increasing concentrations of PF-04691502 for the indicated times. A) Cell viability was measured by means of a resazurin-based cell viability assay. Cell growth curves represent the averages of three independent replicates (n=3). Error bars represent average ± SD for each drug concentration. B) Cell cycle progression was assessed by PI staining followed by flow cytometry analysis. Bar graphs represent the ratio of G1 to (S+G2M) of three independent replicates (n=3). C) Apoptosis was evaluated by flow cytometry of annexin V/DAPI stained cells. Each bar represents the average ± SD percentages of apoptotic cells of three independent replicates (n=3). Statistical analysis was performed by one-way ANOVA followed by Dunnett's multiple comparisons: *p<0.05, **p<0.01, ***p<0.001, ****p<0.0001.

Figure 5. Combination of quizartinib and PF-04691502 synergistically reduces cell viability and induces apoptosis.

A) Cell viability of MOLM-13 cells were exposed to a concentration range of quizartinib (quiz) and PF-04691502 close to IC50 concentrations for 48 hours, either alone or in combination. Heatmaps and bar graphs represent the average percentage of inhibition of cell viability of four independent replicates (n=4). Bar graphs represent average ± SD for each drug concentration. Statistical analysis was performed by student's t-test. Combination index (CI) was calculated by Chou-Talalay and Bliss Independence methods. For CI by Chou-Talalay method CI<1 indicates synergism, CI=1 additive effect, and CI>1 antagonism. CI by Bliss independence method calculated using SynergyFinder (version 2.0) identified synergistic (dark) and antagonistic (light) concentration regions. The most

synergistic area is highlighted with a box. B) Cell cycle state was measured in MOLM-13 cells exposed to an increasing range of concentrations of quizartinib and PF-04691502, close to the drug IC50 concentrations for 48 hours either alone or in combination. Bar graphs represent the ratio of G1 to (S+G2M) of four independent replicates ± SD (n=4). The combination of the highest drug concentration was toxic and therefore not included. C) Apoptosis was measured on MOLM-13 cells exposed to an increasing range of concentrations of quizartinib and PF-04691502, close to the drug IC50 concentrations for 48 hours either alone or in combination. Bar graphs represents the average ± SD of four independent replicates ± SD (n=4). Statistical analysis was performed by unpaired Student's t-test: *$p<0.05$, **$p<0.01$, ***$p<0.001$, ****$p<0.0001$.

Legends for Supplementary Figures and Tables.

Table 1S. IC50 values of human AML cell lines treated with PF-04691502 or quizartinib. IC50 values (nM) represent average of three independent replicates (n=3). 'not reached*' was tested up to 10,000 nM quizartinib.

Figure 1S. FLT3 wild-type and FLT3-ITD AML cell lines display differential sensitivity to PI3K signaling blockade. The effect of addition of increasing concentration of CAL-101, LY-3023414 and PF-04691502 for 48 hours on viability of the indicated AML cell lines was assessed by MTT assays. Values represent the mean of three indipendent replicates (n=3). Statistical analysis was performed by one-way ANOVA followed by Dunnett's multiple comparisons: **p<0.01, ***p<0.001, ****p<0.0001.

Figure 2S. Effect of inhibition of PI3K signaling on cleavage of caspase 7 and PARP in FLT3 wild-type AML cells. The status of the apoptosis markers caspase 7 (upper panel) and PARP (lower panel) in the indicated FLT3 wild-type AML cells treated with either PI3K-p110δ or dual PI3K/mTOR inhibitors LY-3023414 and PF-04691502 was analyzed by RPPA. Time points and concentrations were as indicated. Control samples, treated with drug vehicle only (DMSO), were included at each time point. The results are presented as drug-treated *versus* vehicle-treated cells (%) and are individual values from four replicates showing <5% deviation.

.

Figure 3S. AKT phosphorylation in FLT3 wild-type AML cells. As a readout of PI3K signaling inhibition activation, AKT S473 phosphorylation was analyzed through RPPA, in FLT3 wild-type

AML cells treated with ether PI3K-p110δ or dual PI3K/mTOR inhibitors. The concentrations were as indicated. The RPPA experimental design included three time points, i.e. 1, 16 and 48 hours. Control samples, i.e. cells treated with drug vehicle only (DMSO), were included at each time point. The results are presented as drug-treated *versus* vehicle-treated cells (%) and are individual values from four replicates showing <5% deviation.

A

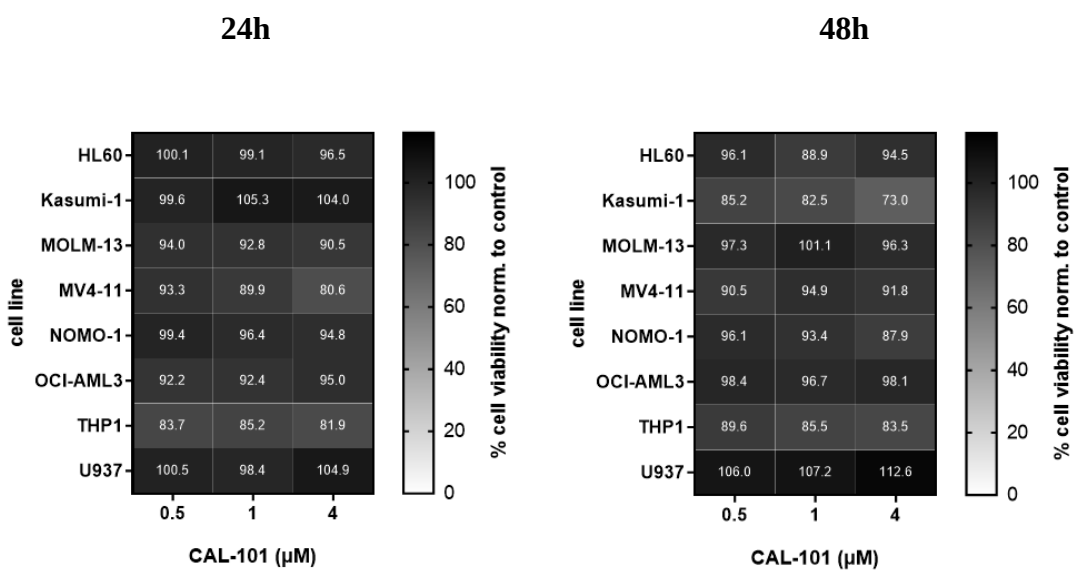
24h
48h
cell line
HL60
Kasumi-1
MOLM-13
MV4-11
NOMO-1
OCI-AML3
THP1
U937
100.1 99.1 96.5
99.6 105.3 104.0
94.0 92.8 90.5
93.3 89.9 80.6
99.4 96.4 94.8
92.2 92.4 95.0
83.7 85.2 81.9
100.5 98.4 104.9
96.1 88.9 94.5
85.2 82.5 73.0
97.3 101.1 96.3
90.5 94.9 91.8
96.1 93.4 87.9
98.4 96.7 98.1
89.6 85.5 83.5
106.0 107.2 112.6
0.5 1 4
CAL-101 (µM)
% cell viability norm. to control
100 80 60 40 20 0

B

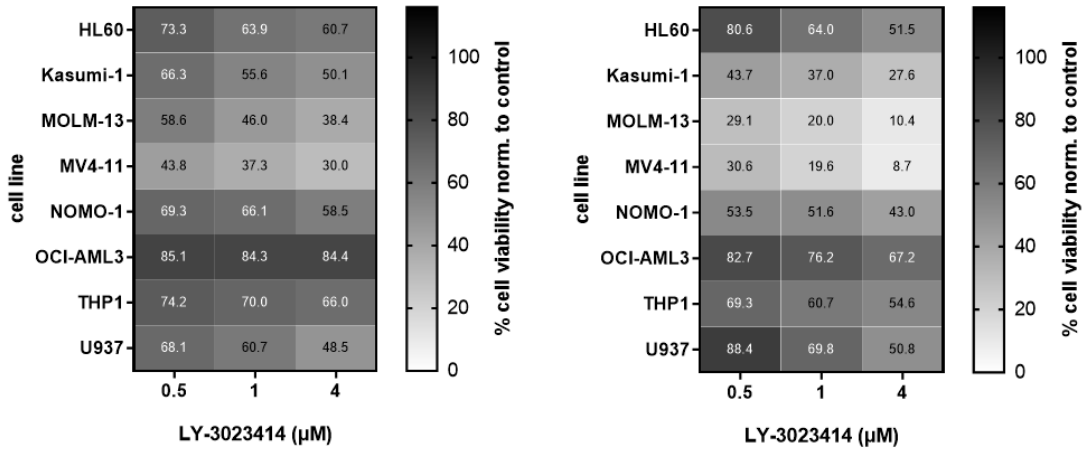
cell line
HL60
Kasumi-1
MOLM-13
MV4-11
NOMO-1
OCI-AML3
THP1
U937
73.3 63.9 60.7
66.3 55.6 50.1
58.6 46.0 38.4
43.8 37.3 30.0
69.3 66.1 58.5
85.1 84.3 84.4
74.2 70.0 66.0
68.1 60.7 48.5
80.6 64.0 51.5
43.7 37.0 27.6
29.1 20.0 10.4
30.6 19.6 8.7
53.5 51.6 43.0
82.7 76.2 67.2
69.3 60.7 54.6
88.4 69.8 50.8
0.5 1 4
LY-3023414 (µM)
% cell viability norm. to control
100 80 60 40 20 0

C

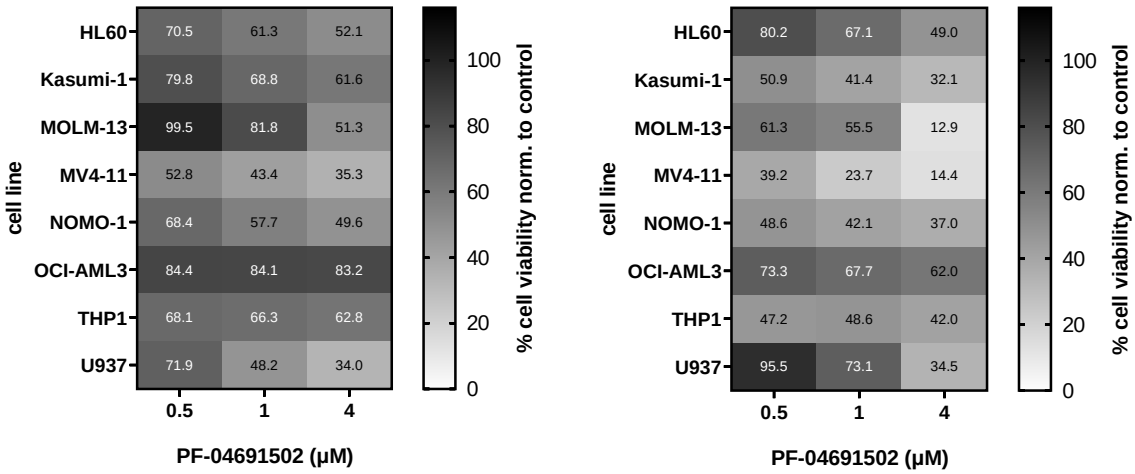
HL60
Kasumi-1
MOLM-13
MV4-11
NOMO-1
OCI-AML3
THP1
U937
cell line
70.5 61.3 52.1
79.8 68.8 61.6
99.5 81.8 51.3
52.8 43.4 35.3
68.4 57.7 49.6
84.4 84.1 83.2
68.1 66.3 62.8
71.9 48.2 34.0
0.5 1 4
PF-04691502 (µM)
100 80 60 40 20 0
% cell viability norm. to control
80.2 67.1 49.0
50.9 41.4 32.1
61.3 55.5 12.9
39.2 23.7 14.4
48.6 42.1 37.0
73.3 67.7 62.0
47.2 48.6 42.0
95.5 73.1 34.5

Figure 1

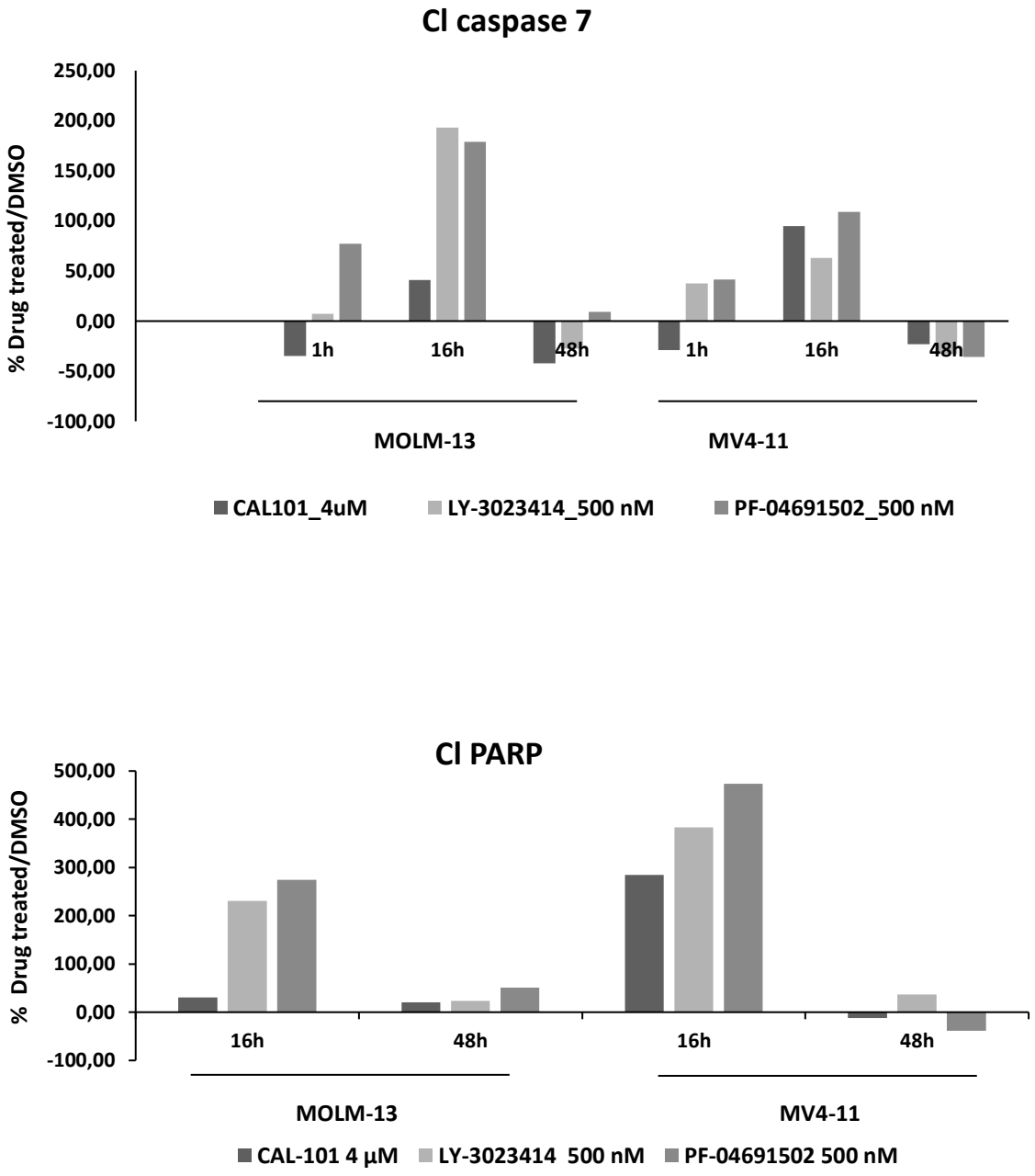
Cl caspase 7
% Drug treated/DMSO
250,00
200,00
150,00
100,00
50,00
0,00
-50,00
-100,00
1h
16h
48h
1h
16h
48h
MOLM-13
MV4-11
CAL101_4uM
LY-3023414_500 nM
PF-04691502_500 nM
Cl PARP
% Drug treated/DMSO
500,00
400,00
300,00
200,00
100,00
0,00
-100,00
16h
48h
16h
48h
MOLM-13
MV4-11
CAL-101 4 µM
LY-3023414 500 nM
PF-04691502 500 nM

Figure 2

A

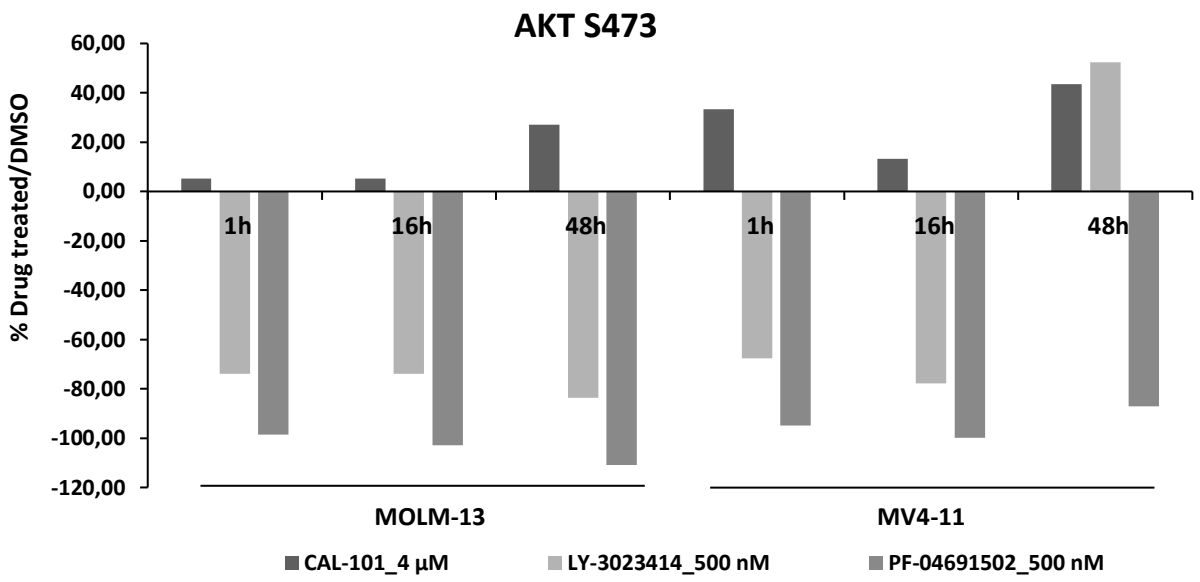
AKT S473
60,00
40,00
20,00
0,00
-20,00
-40,00
-60,00
-80,00
-100,00
-120,00
% Drug treated/DMSO
1h
16h
48h
1h
16h
48h
MOLM-13
MV4-11
CAL-101_4 µM
LY-3023414_500 nM
PF-04691502_500 nM

B

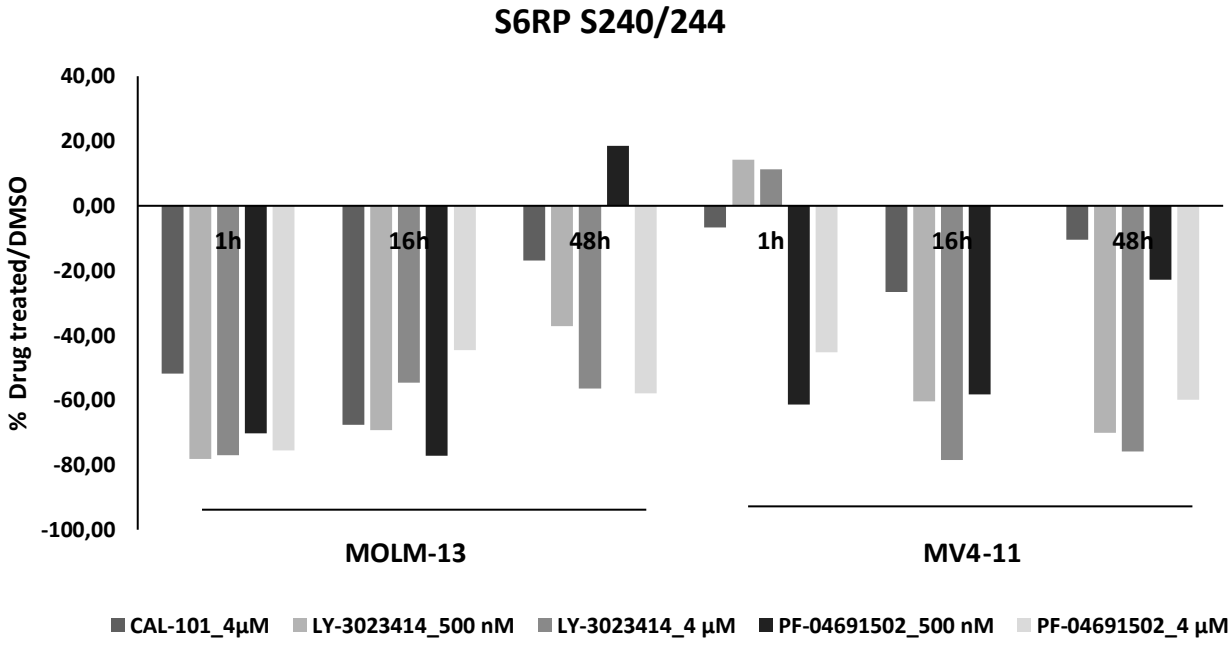
S6RP S240/244
40,00
20,00
0,00
-20,00
-40,00
-60,00
-80,00
-100,00
% Drug treated/DMSO
1h
16h
48h
1h
16h
48h
MOLM-13
MV4-11
CAL-101_4µM
LY-3023414_500 nM
LY-3023414_4 µM
PF-04691502_500 nM
PF-04691502_4 µM

C

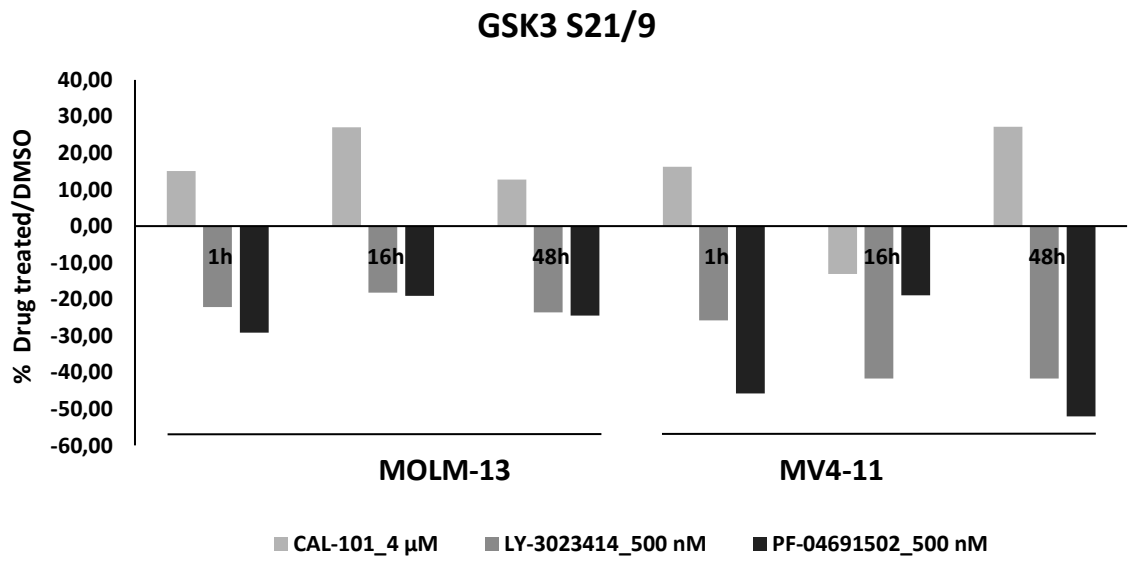
GSK3 S21/9
40,00
30,00
20,00
10,00
0,00
-10,00
-20,00
-30,00
-40,00
-50,00
-60,00
% Drug treated/DMSO
1h
16h
48h
1h
16h
48h
MOLM-13
MV4-11
CAL-101_4 µM
LY-3023414_500 nM
PF-04691502_500 nM

Figure 3

A

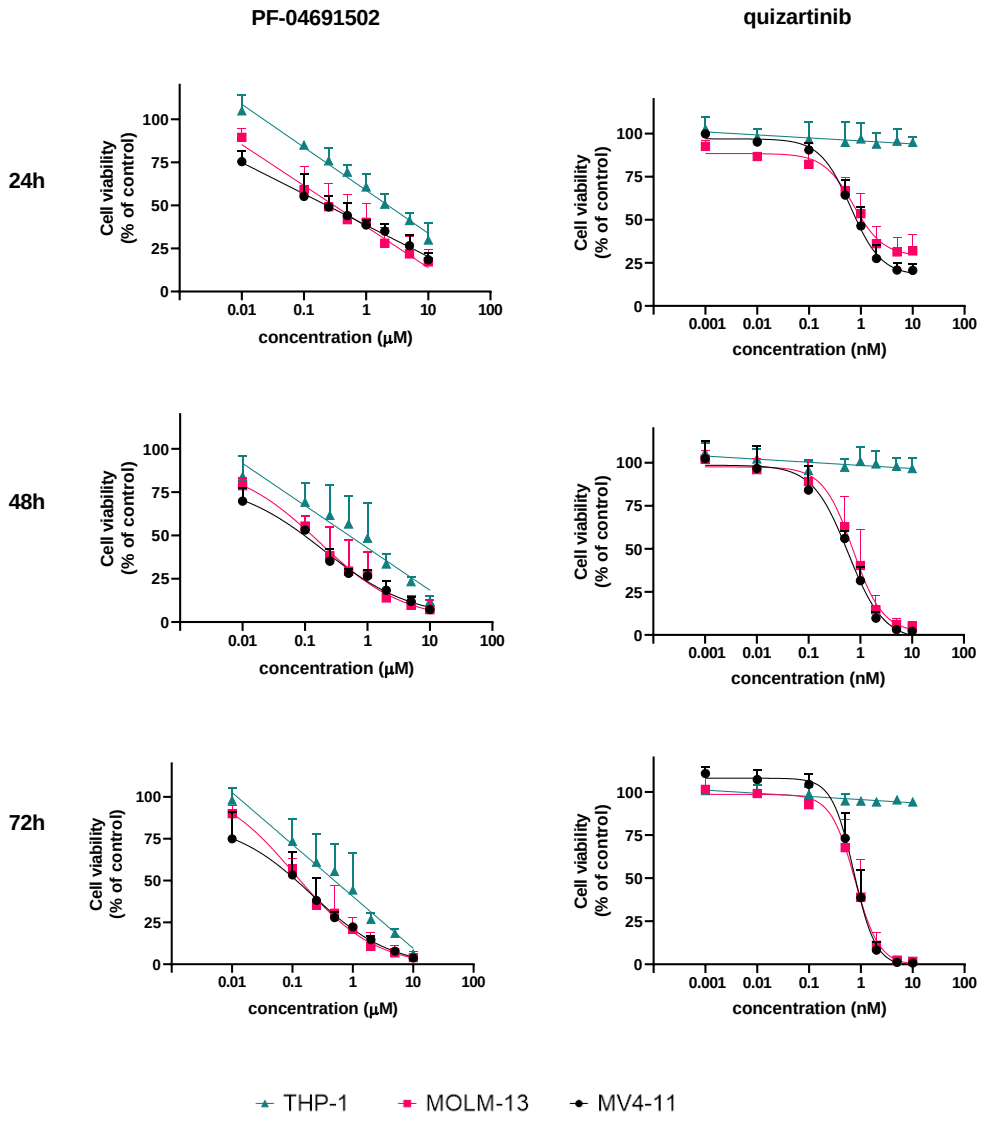
PF-04691502
quizartinib
24h
48h
72h
Cell viability (% of control)
concentration (μM)
concentration (nM)
0
25
50
75
100
0.01
0.1
1
10
0.001
THP-1
MOLM-13
MV4-11

B

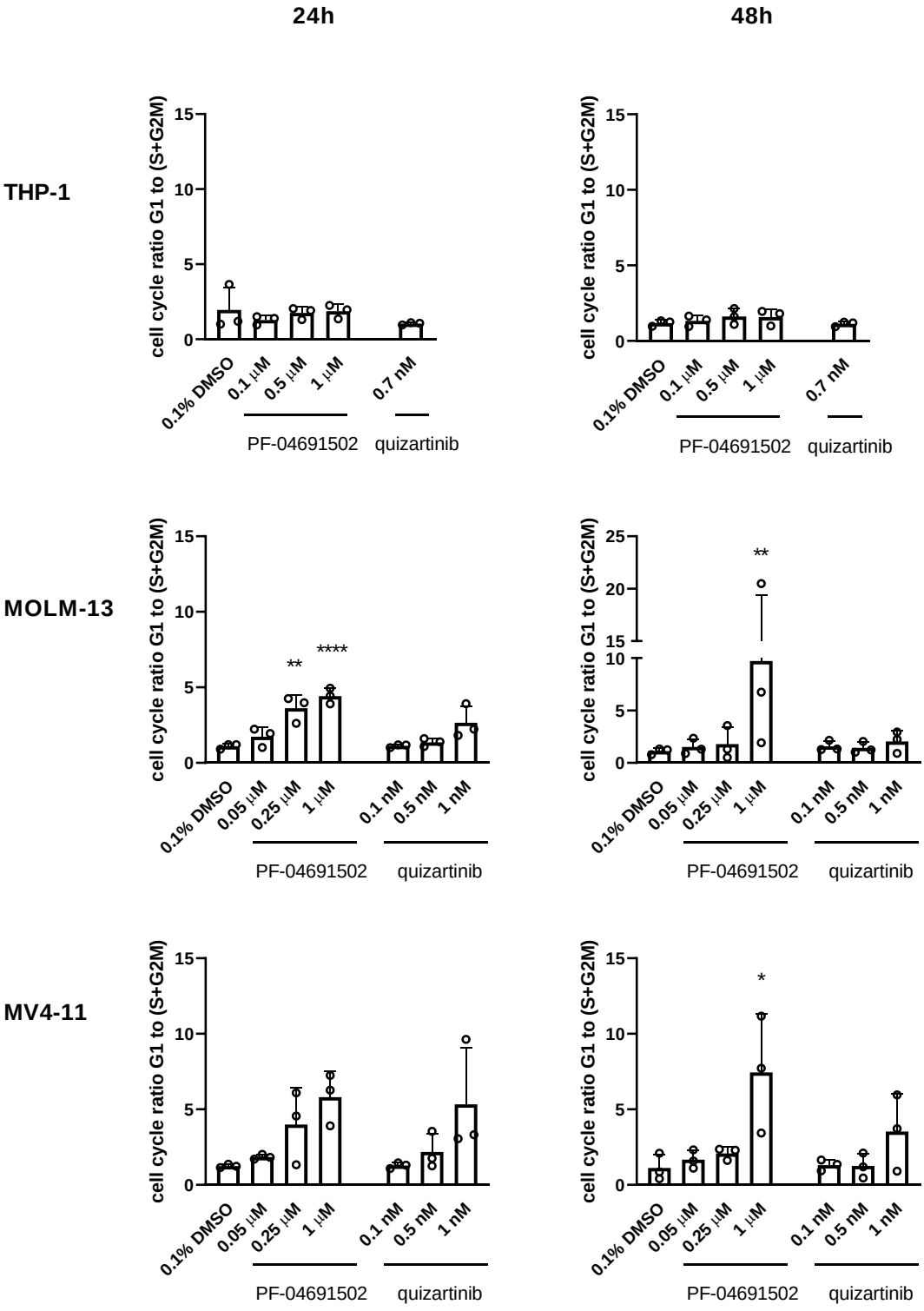
24h
48h
THP-1
MOLM-13
MV4-11
cell cycle ratio G1 to (S+G2M)
0.1% DMSO
0.1 μM
0.5 μM
1 μM
0.7 nM
0.05 μM
0.25 μM
0.1 nM
0.5 nM
1 nM
PF-04691502
quizartinib
**
****
*

C

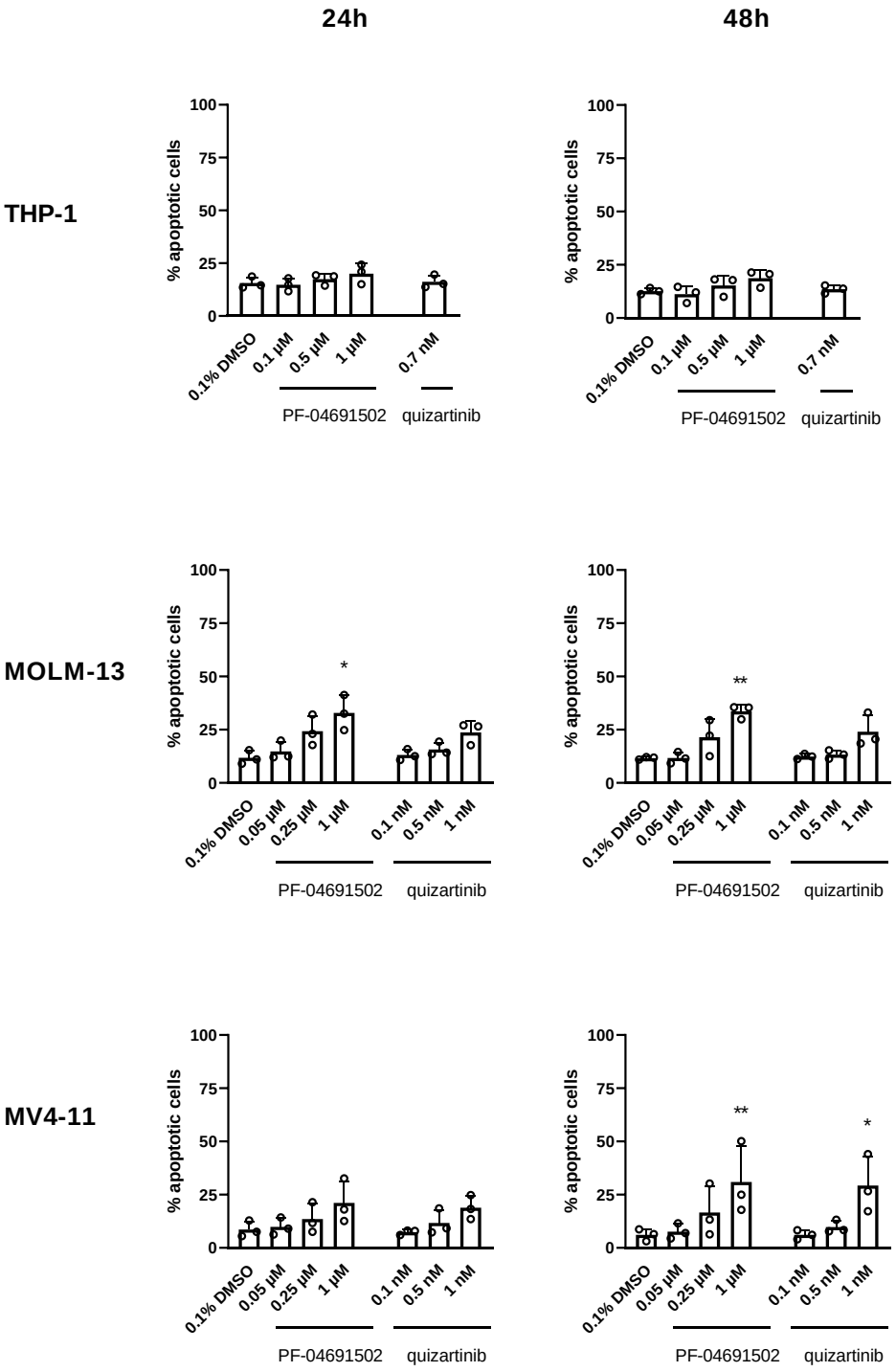
24h
48h
THP-1
MOLM-13
MV4-11
% apoptotic cells
100
75
50
25
0
0.1% DMSO
0.1 µM
0.5 µM
1 µM
0.7 nM
0.05 µM
0.25 µM
0.1 nM
0.5 nM
1 nM
PF-04691502
quizartinib
*
**

Figure 4.

A

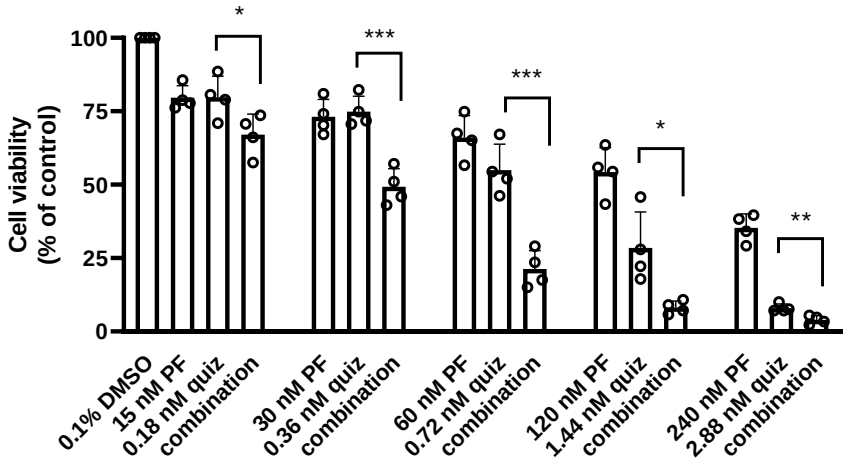
Cell viability
(% of control)
100
75
50
25
0
*
***
***
*
**
0.1% DMSO
15 nM PF
0.18 nM quiz
combination
30 nM PF
0.36 nM quiz
combination
60 nM PF
0.72 nM quiz
combination
120 nM PF
1.44 nM quiz
combination
240 nM PF
2.88 nM quiz
combination

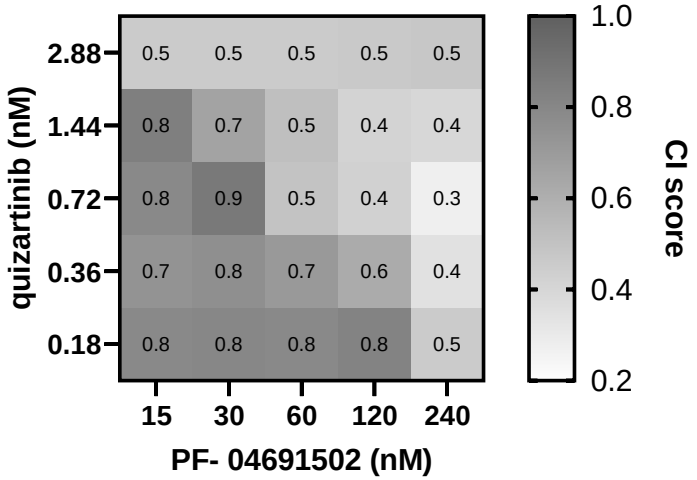
quizartinib (nM)
2.88
1.44
0.72
0.36
0.18
0.5 0.5 0.5 0.5 0.5
0.8 0.7 0.5 0.4 0.4
0.8 0.9 0.5 0.4 0.3
0.7 0.8 0.7 0.6 0.4
0.8 0.8 0.8 0.8 0.5
15 30 60 120 240
PF- 04691502 (nM)
1.0
0.8
0.6
0.4
0.2
CI score

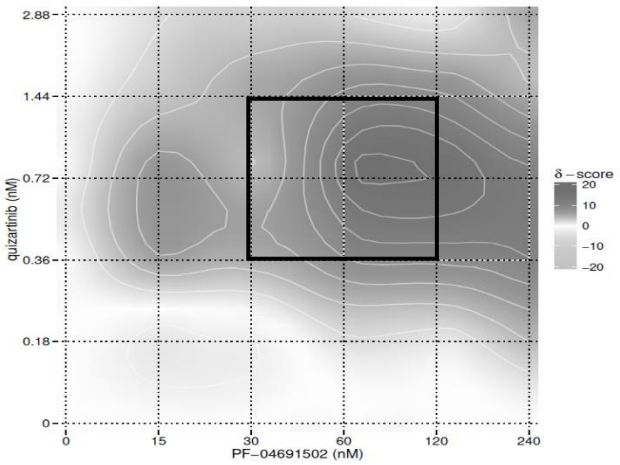
quizartinib (nM)
2.88
1.44
0.72
0.36
0.18
0
0 15 30 60 120 240
PF−04691502 (nM)
δ − score
20
10
0
−10
−20

B

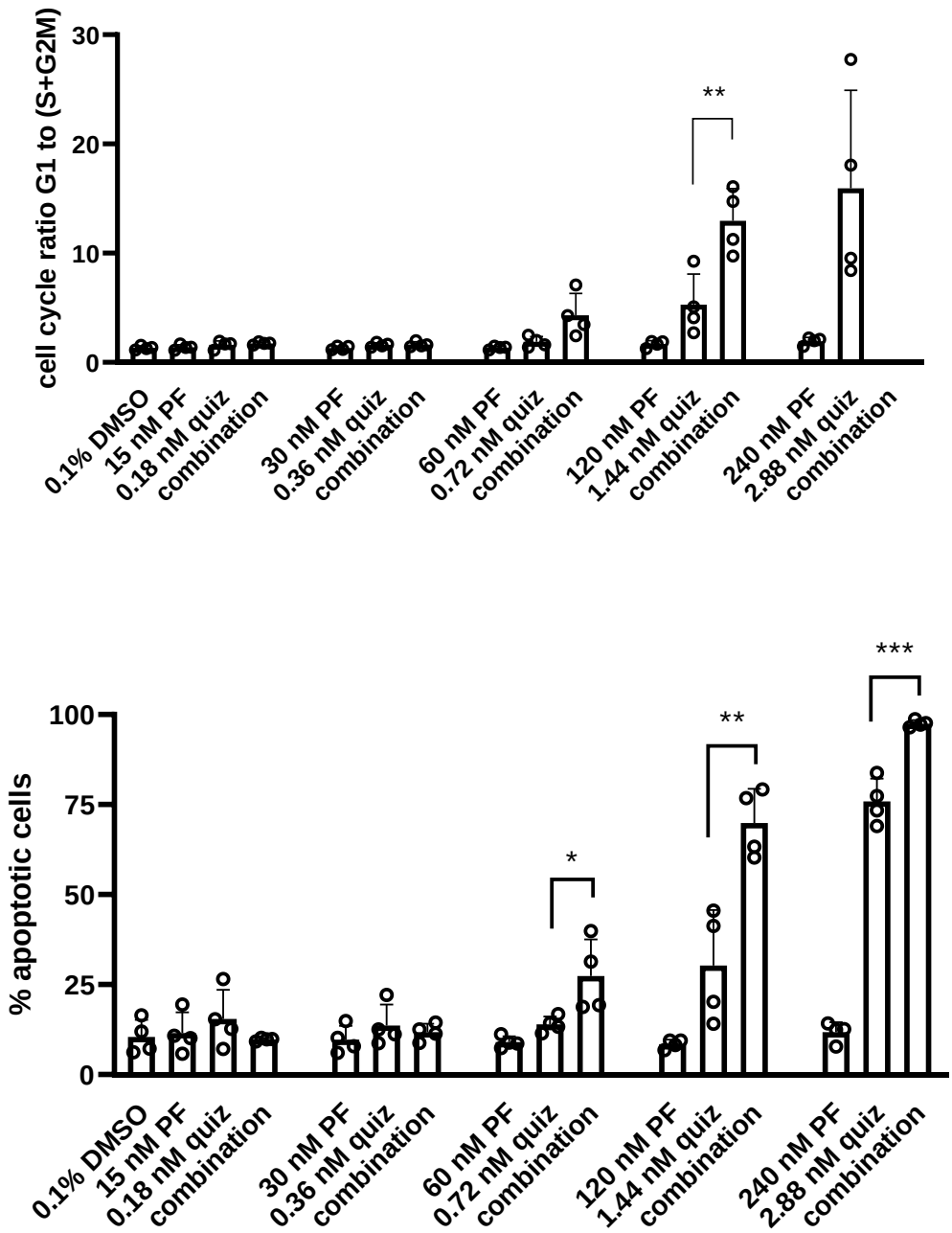
cell cycle ratio G1 to (S+G2M)
30
20
10
0
**
0.1% DMSO
15 nM PF
0.18 nM quiz
combination
30 nM PF
0.36 nM quiz
combination
60 nM PF
0.72 nM quiz
combination
120 nM PF
1.44 nM quiz
combination
240 nM PF
2.88 nM quiz
combination
% apoptotic cells
100
75
50
25
0
*
**
***
0.1% DMSO
15 nM PF
0.18 nM quiz
combination
30 nM PF
0.36 nM quiz
combination
60 nM PF
0.72 nM quiz
combination
120 nM PF
1.44 nM quiz
combination
240 nM PF
2.88 nM quiz
combination

Figure 5.

Supplementary Figures.

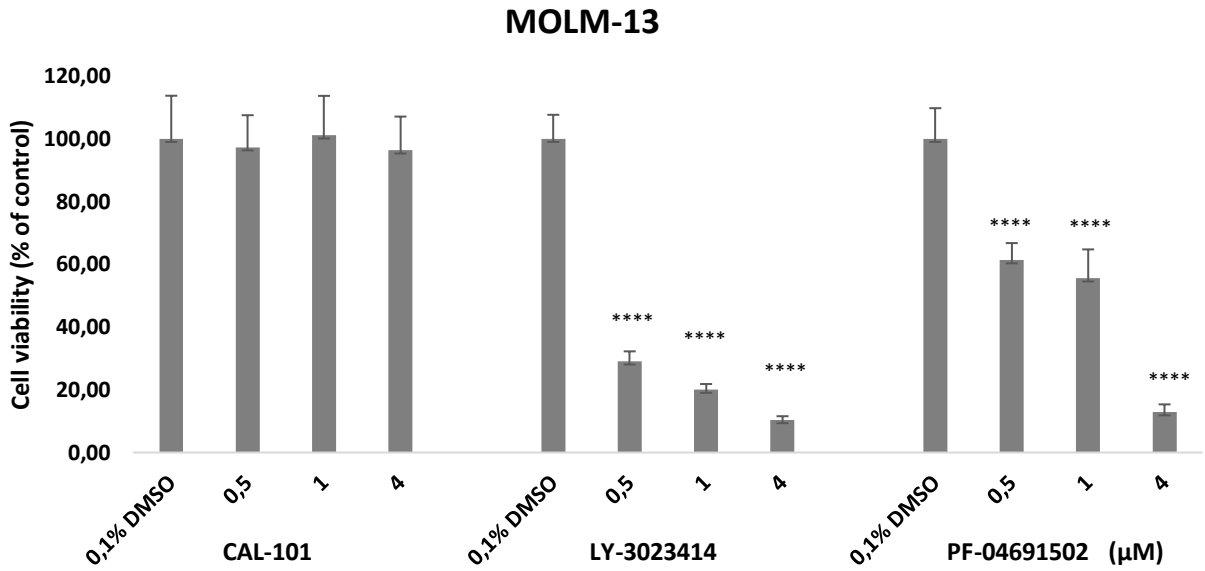

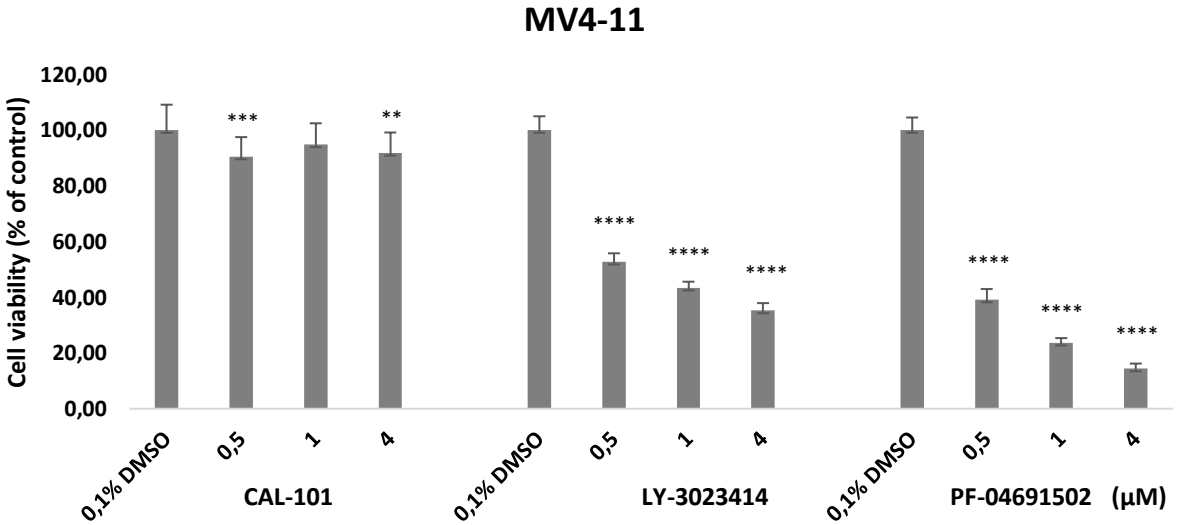

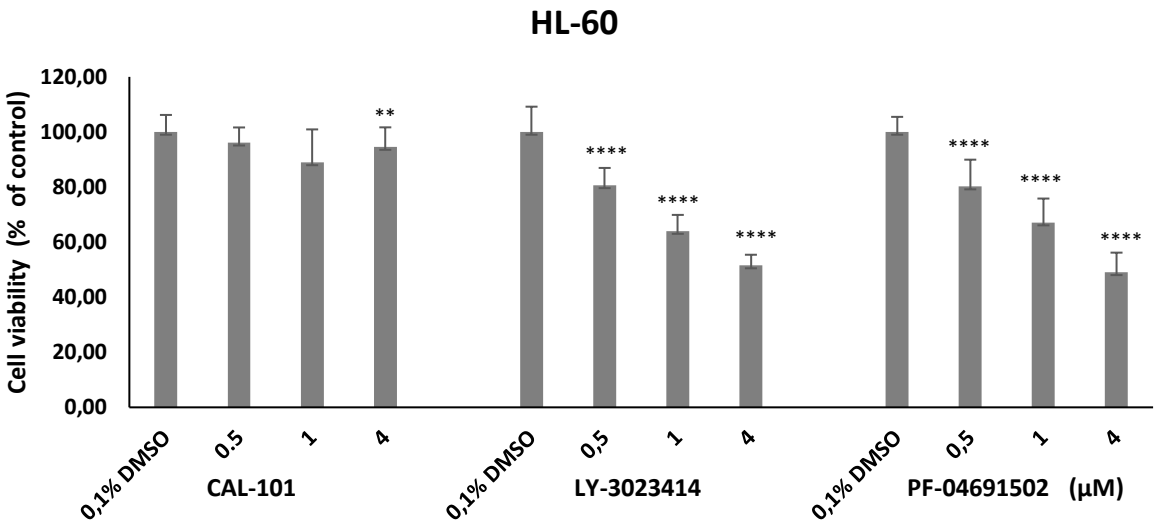
HL-60
Cell viability (% of control)
120,00
100,00
80,00
60,00
40,00
20,00
0,00
**
****
****
****
****
****
****
0,1% DMSO
0,5
1
4
CAL-101
0,1% DMSO
0,5
1
4
LY-3023414
0,1% DMSO
0,5
1
4
PF-04691502 (µM)

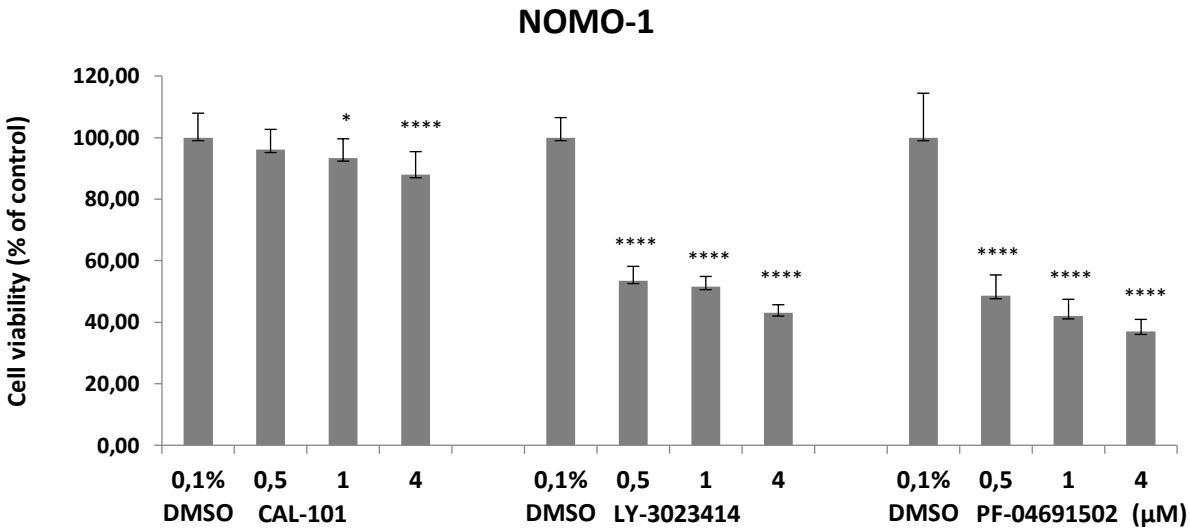
NOMO-1
Cell viability (% of control)
120,00
100,00
80,00
60,00
40,00
20,00
0,00
*
****
****
****
****
****
****
0,1% DMSO
0,5
1
4
CAL-101
0,1% DMSO
0,5
1
4
LY-3023414
0,1% DMSO
0,5
1
4
PF-04691502 (µM)

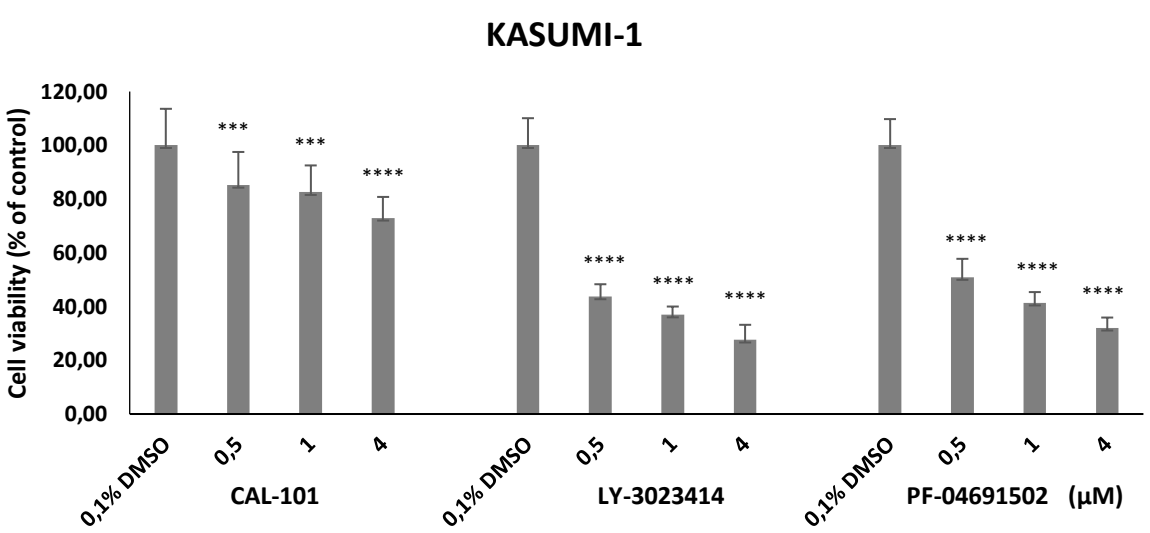
KASUMI-1
Cell viability (% of control)
120,00
100,00
80,00
60,00
40,00
20,00
0,00
***
***
****
****
****
****
****
****
****
0,1% DMSO
0,5
1
4
CAL-101
0,1% DMSO
0,5
1
4
LY-3023414
0,1% DMSO
0,5
1
4
PF-04691502 (µM)

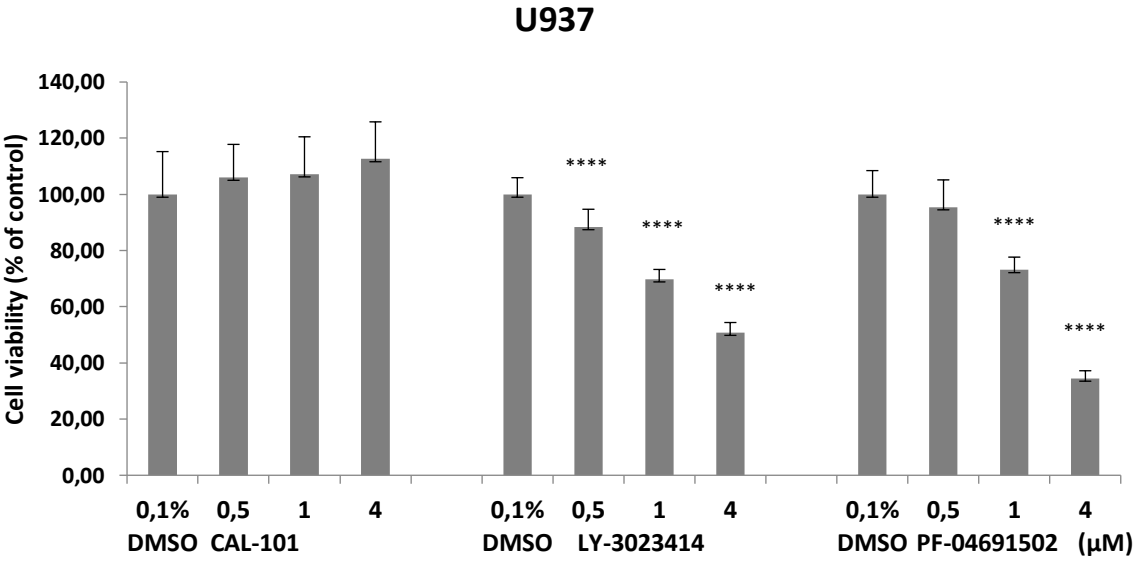
U937
Cell viability (% of control)
140,00
120,00
100,00
80,00
60,00
40,00
20,00
0,00
****
****
****
****
****
****
0,1% DMSO
0,5
1
4
CAL-101
0,1% DMSO
0,5
1
4
LY-3023414
0,1% DMSO
0,5
1
4
PF-04691502 (µM)

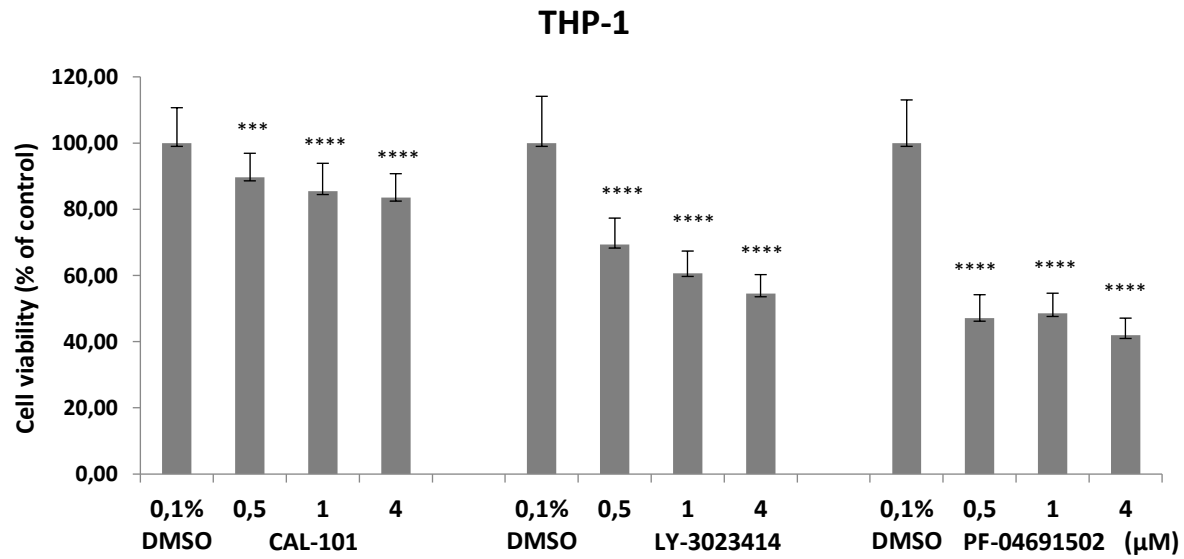
THP-1
Cell viability (% of control)
120,00
100,00
80,00
60,00
40,00
20,00
0,00
***
****
0,1% 0,5 1 4
DMSO CAL-101
LY-3023414
PF-04691502 (μM)

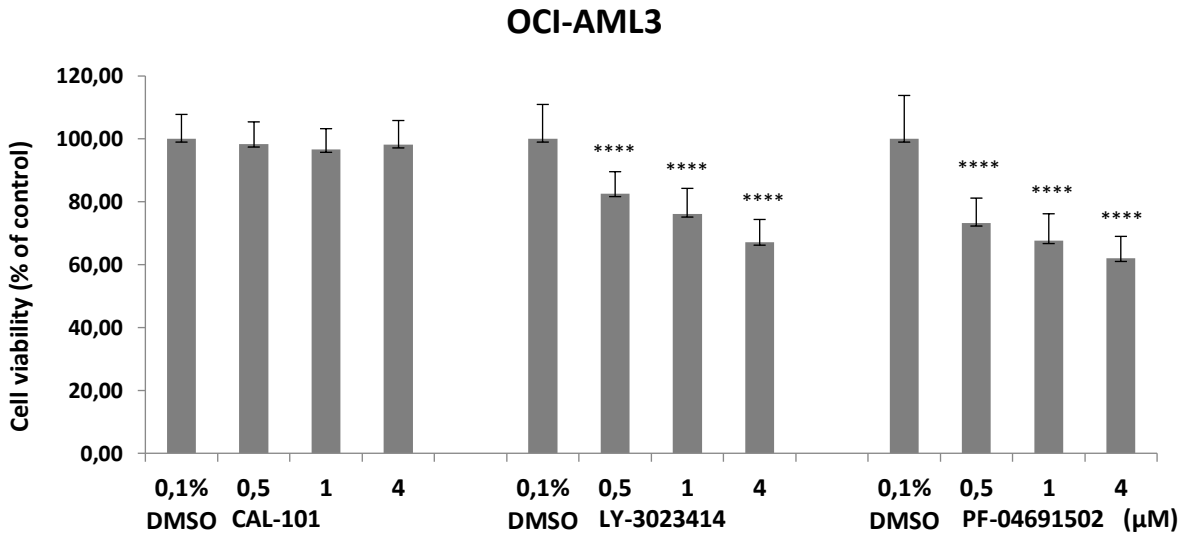
OCI-AML3
Cell viability (% of control)
120,00
100,00
80,00
60,00
40,00
20,00
0,00
****
0,1% 0,5 1 4
DMSO CAL-101
LY-3023414
PF-04691502 (μM)

Figure 1S.

Cell line	Compound	24h	48h	72h
THP-1	PF-04691502	2252.6	508.3	497.8
	quizartinib	not reached*	not reached*	not reached*
MOLM-13	PF-04691502	304.8	160.9	111.1
	quizartinib	0.7	0.7	0.8
MV4-11	PF- 04691502	233.9	195.4	206.8
	quizartinib	0.6	0.6	0.7

Table 1S.

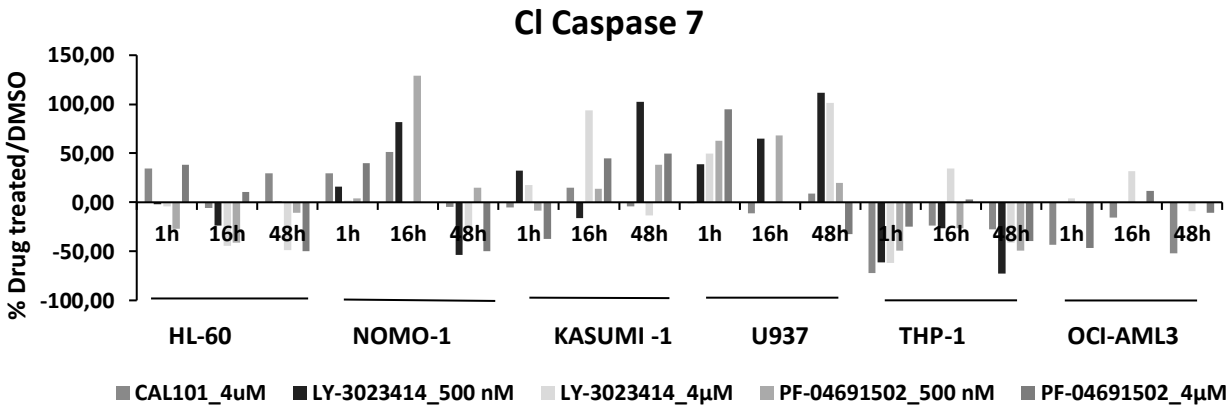

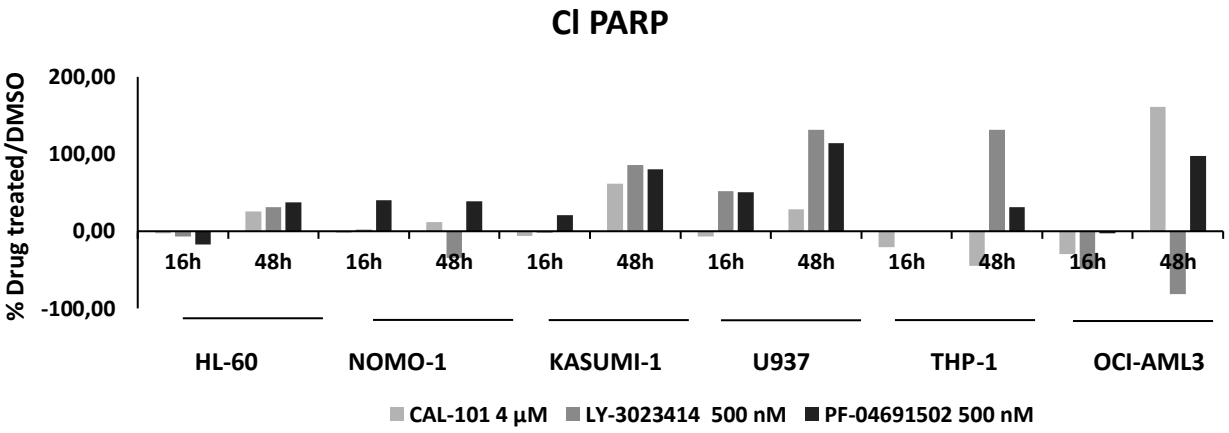
Cl PARP
% Drug treated/DMSO
200,00
100,00
0,00
-100,00
16h
48h
HL-60
NOMO-1
KASUMI-1
U937
THP-1
OCI-AML3
CAL-101 4 µM
LY-3023414 500 nM
PF-04691502 500 nM

Figure 2S

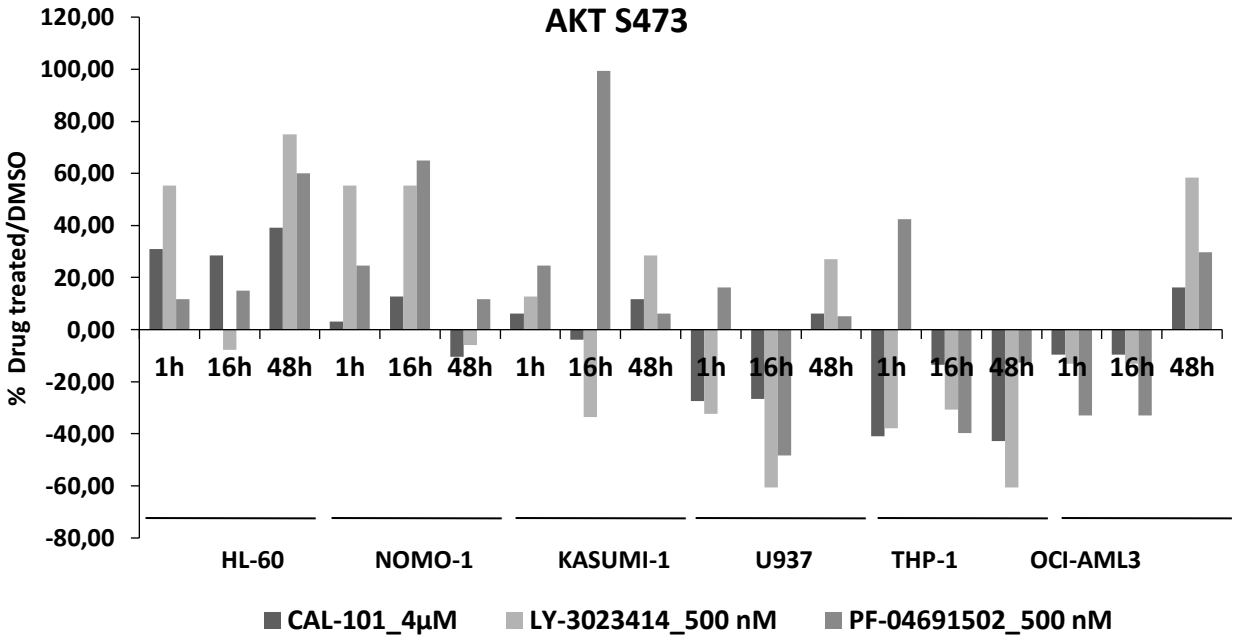
AKT S473
120,00
100,00
80,00
60,00
40,00
20,00
0,00
-20,00
-40,00
-60,00
-80,00
% Drug treated/DMSO
1h 16h 48h 1h 16h 48h 1h 16h 48h 1h 16h 48h 1h 16h 48h 1h 16h 48h
HL-60
NOMO-1
KASUMI-1
U937
THP-1
OCI-AML3
CAL-101_4µM
LY-3023414_500 nM
PF-04691502_500 nM

Figure 3S